Hydraulics and drones: observations of water level, bathymetry and water surface velocity from Unmanned Aerial Vehicles

Bandini, Filippo; Bauer-Gottwein, Peter; Garcia, Monica

Publication date:
2017

Document Version
Publisher's PDF, also known as Version of record

Hydraulics and drones: observations of water level, bathymetry and water surface velocity from Unmanned Aerial Vehicles.

Filippo Bandini

PhD Thesis
December 2017

DTU Environment
Department of Environmental Engineering

Hydraulics and drones: observations of water level, bathymetry and water surface velocity from Unmanned Aerial Vehicles.

Filippo Bandini

PhD Thesis
December 2017

DTU Environment
Department of Environmental Engineering
Technical University of Denmark

PhD project: Environmental monitoring with unmanned aerial vehicles

Filippo Bandini

PhD Thesis, December 2017

Address: DTU Environment
Department of Environmental Engineering
Technical University of Denmark
Miljoevej, building 113
2800 Kgs. Lyngby
Denmark

Phone reception: +45 4525 1600
Fax: +45 4593 2850

Homepage: http://www.env.dtu.dk
E-mail: reception@env.dtu.dk

Cover: GraphicCo

Preface

The work presented in this PhD thesis was conducted at the Department of Environmental Engineering, Technical University of Denmark, from May 2014 to August 2017 under the supervision of Professor Peter Bauer-Gottwein and co-supervisor Assistant Professor Monica Garcia. The Innovation Fund Denmark is acknowledged for providing funding for this PhD project via the project Smart UAV [125-2013-5]. Four scientific papers constitute the PhD work presented herein. The papers are listed below and will be referred to using the Roman numerals **I-IV** throughout the thesis.

I **Bandini, F.**, Jakobsen, J., Olesen, D., Reyna-Gutierrez, J. A., and Bauer-Gottwein, P. (2017). "Measuring water level in rivers and lakes from lightweight Unmanned Aerial Vehicles." *Journal of Hydrology*, 548, 237–250

II **Bandini, F.**, Butts, M., Vammen Torsten, J., and Bauer-Gottwein, P. (2017). "Water level observations from Unmanned Aerial Vehicles for improving estimates of surface water-groundwater interaction". *In print-Hydrological Processes*.

III **Bandini, F.**, Olesen, D., Jakobsen, J., Kittel, C. M. M., Wang, S., Garcia, M., and Bauer-Gottwein, P. (2017). "River bathymetry observations from a tethered single beam sonar controlled by an Unmanned Aerial Vehicle." *Manuscript under review.*

IV **Bandini, F.**, Lopez-Tamayo, A., Merediz-Alonso, G., Olesen, D., Jakobsen, J., Wang, S., Garcia, M., and Bauer-Gottwein, P. (2017). "Unmanned Aerial Vehicle observations of bathymetry and water level in the cenotes and lagoons of the Yucatan Peninsula". *Manuscript under review.*

TEXT FOR WWW-VERSION (without papers)

In this online version of the thesis, paper **I-IV** are not included but can be obtained from electronic article databases e.g. via www.orbit.dtu.dk or on request from DTU Environment, Technical University of Denmark, Miljoevej, Building 113, 2800 Kgs. Lyngby, Denmark, info@env.dtu.dk.

In addition, the following publications, not included in this thesis, were also co-authored during this PhD study:

Wang, S., **Bandini, F.**, Dam-Hansen, C., Thorseth, A., Zarco-Tejada, P. J., Jakobsen, J., Ibrom, A., Bauer-Gottwein, P., and Garcia, M. (2017). Optimizing sensitivity of Unmanned Aerial System optical sensors for low irradiance and cloudy conditions. *Manuscript in preparation*.

Wang, S., **Bandini, F.**, Jakobsen, J., Ibrom, A., J. Zarco Tejada, P., Bauer-Gottwein, P., and Garcia., M. (2017). A continuous hyperspatial monitoring system of evapotranspiration and gross primary productivity from Unmanned Aerial Systems. *Manuscript in preparation*.

Christian, K., **Bandini, F.**, Wang, S., García, M., Bauer-Gottwein, P. (2016). Applying drones for thermal detection of contaminated groundwater influx (Grindsted Å). Appendix in *Anvendelse af drone til termisk kortlægning af forureningsudstrømning*. Report of Drone System (Henrik Grosen, Sune Nielsen), edited by Miljøstyrelsen.

Acknowledgements

I would like to thank my main supervisor Professor Peter Bauer-Gottwein for his support throughout the 3 years of this PhD, keeping me going when times were tough, asking insightful questions, and offering invaluable advice. Thanks for having made it possible to achieve.

I thank my co-supervisor Assistant Professor Monica Garcia for her continued support and guidance from day one. I remember being teaching assistant with her as a very nice academic experience.

Special thanks to Jakob Jakobsen, unofficial co-supervisor from DTU space, for the time spent to help and support me, for the first flights and campaigns conducted together, for the scientific discussions in the lab or in the field and for the success stories we shared.

Many thanks to Daniel Olesen, PhD student at DTU Space, for his invaluable support in the world of Embedded Electronics and his insightful friendship.

I am very grateful to Sheng Wang, PhD student at DTU ENV, for the flight campaigns conducted together in DTU Risø or Lille Skensved, for the time spent together and for his invaluable friendship.

I need to mention all the students who have collaborated with me in this project. I thank: Christian Josef Köppl for his help, his support and for his problem solving skills; Lars Ørsøe for the initial work we conducted together on integrating and calibrating the thermal and multispectral cameras; Benjamin Holm and Rasmus Goosmann for their project about measuring surface water speed from UAVs; Veronica Sobejando Paz for her valuable master's thesis and for the field campaigns conducted together.

A huge and warm thank also to my colleagues of the WRE section, including Klaus, Biao, Claus, Cecile, Raphael, Grith, Anne, Alex, Lucian, Liguang, Vinni, Nicola, Maria, Pernille, Kawawa, Louise, Mkhuzo, etc… You turned difficult days into fun ones and make happy days even happier.

Summary

The planet faces several water-related threats, including water scarcity, floods, and pollution. Satellite and airborne sensing technology is rapidly evolving to improve the observation and prediction of surface water and thus prevent natural disasters. While technological developments require extensive research and funding, they are far less expensive and therefore more important than disaster restoration and remediation. Thus, our research question was “Can we retrieve hydraulic observations of inland surface water bodies, whenever and wherever it is required, with (i) high accuracy, (ii) high spatial resolution and (iii) at a reasonable cost?”. Unmanned Aerial Vehicles (UAVs) and their miniaturized components can solve this challenge. Indeed, they can monitor dangerous or difficult-to-reach areas delivering real time data. Furthermore, they ensure high accuracy and spatial resolution in monitoring surface water bodies, at a limited cost and with high flexibility.

This PhD project investigates and demonstrates how UAVs can enrich the set of available hydraulic observations in inland water bodies, including:

1. Orthometric water level
2. Water depth (bathymetry)
3. Surface water speed

The novelty of this research is to retrieve water level and bathymetry measurements from UAVs. The objective is to retrieve these observations with an accuracy of few cm, without any need for GCPs (Ground Control Points), and without any dependency on river morphology, water turbidity, and maximum water depth. Although UAV-borne measurements of surface water speed have already been documented in the literature, a novel approach was developed to avoid GCPs.

This research is the first demonstration that orthometric water level can be measured from UAVs with a radar system and a GNSS (Global Navigation Satellite System) receiver. As in satellite altimetry, the GNSS receiver measures the altitude above mean sea level, while the radar measures the range to the water surface. The orthometric water level is then computed by subtracting the range measured by the radar from the GNSS-derived altitude. However, compared to satellites, UAVs have several advantages: high spatial resolution, repeatability of the flight missions and good tracking of the water

bodies. Nevertheless, UAVs face several constraints: vibrations, limited size, weight, and electric power available for the sensors. In this thesis, we present the first studies on UAV altimetry. Studies were conducted to measure orthometric water level (height of water surface above sea mean level) in rivers, lakes, and in the worldwide unique cenotes and lagoons of the Yucatan peninsula. An accuracy of ca. 5-7 cm is achievable with our technology. This accuracy is higher than any other spaceborne radar or spaceborne LIDAR altimeter.

Water depths were measured by UAV with a tethered sonar controlled by the UAV. Bathymetry can be estimated by subtracting water depth from water level. Our technology aims to combine the large spatial and temporal coverage capabilities of remote sensing techniques, with the accuracy of in-situ measurements. An accuracy of ca. 2.1% of the actual depth was achieved with our system, with a maximum depth capability potentially up to 80 m. Since remote sensing techniques (e.g LIDARs, through-water photogrammetry, spectral-depth signature of multispectral imagery) can survey water depths up to few meters only, our technology has a maximum depth capability and an applicability range superior to any other remote sensing technique. Compared to manned or unmanned vessels equipped with echo sounders, our UAV-borne technology can also survey non-navigable rivers and overpass obstacles (e.g. river structures). Computer vision, autopilot system and beyond visual line-of-sight (BVLOS) flights will ensure the possibility to retrieve hyper-spatial observations of water depth, without requiring the operator to access the area.

Surface water speed can be measured with UAVs using image cross correlation techniques. UAV-borne water speed observations can overcome the practical difficulties of traditional methods. Indeed flow measurements are often intrusive (e.g. flow meters) or require deployment of vessels equipped with expensive acoustic Doppler current profilers (ADCPs). For these reasons, water speed observations have been traditionally challenging, especially in difficult-to-access environments. Conversely, UAV-borne observations open up the possibility of measuring water speed over extended regions at a low cost. The 2D water surface velocity field is computed by analysing the UAV-borne video frames using a technique called large scale PIV (Particle Image Velocimetry). PIV is well known in micro scale applications, but large scale PIV faces several challenges. For instance, it is not possible to use laser systems to better illuminate the water surface. Our preliminary studies show that UAVs can measure surface water speed of rivers. However, seeding of the

water surface is required due to the lack of natural tracers (e.g. bubbles, debris, and foam) occurring in the Danish free-flowing rivers. Furthermore, video stabilization techniques are essential to remove the effects of drone vibrations. An innovative procedure was adopted to convert from image units (pixels) into metric units, by using the on-board radar observations.

A study was conducted to evaluate the potential of UAV-borne water observations for calibrating a hydrological model. The hydrological model simulates Mølleåen river (Denmark) and its catchment. The model-derived estimates of groundwater-surface water (GW-SW) interaction were significantly improved after calibration against synthetic UAV-borne observations. After calibration against UAV-borne water level observations, the sharpness (width of the confidence interval) of GW-SW time series is improved by ca. 50%, RMSE (Root Mean Square Error) decreases by ca. 75%, and the direction of the GW-SW flux is better simulated.

Dansk sammenfatning

Jorden er truet af mange forskellige vandrelaterede hændelser, såsom tørke, oversvømmelser og forurening. Satellit- og luftbåren måleteknik udvikler sig hurtigt og giver nye muligheder for at indhente observationer af overfladevand for derigennem at hindre naturkatastrofer. Teknologisk udvikling kræver udstrakt forskning med tilhørende bevillinger, men er dog langt billigere end udgifterne til nødhjælp og genopretning efter katastrofer. Det spørgsmål, der blev stillet, var: ”Er det muligt at opnå hydrauliske observationer af indlands vandområder, hvor og hvornår det er påkrævet, med (i) høj nøjagtighed, (ii) høj rumlig opløsning og (iii) til en overkommelig pris?” Ubemandede lutfartøjer og deres miniature-komponenter kan løse problemet. De kan faktisk foretage målinger i farlige og svært tilgængelige områder i realtid. De kan ydermere tilsikre høj nøjagtighed og høj rumlig opløsning i monitering af overfladevandssystemer til en begrænset omkostning og med en høj grad af fleksibilitet.

Formålet med ph.d.-projektet har været at undersøge og demonstrere, hvordan UAVs kan supplere og forøge de hidtil tilgængelige hydrologiske observationer af indlands overfladevandssystemer, herunder

1. Ortometrisk vandniveau

2. Vanddybde

3. Overfladevandshastighed

Nyskabelsen i denne forskning består i at vandstand- og dybdemålinger opnås ved hjælp UAV’er. Studiets formål var at opnå en præcision på et par cm uden behov for GCP (eng: Ground Control Points) og uafhængigt af flodmorfologi, vandturbiditet eller maksimum vanddybde. Selv om UAV-bårne målinger af overfladevandshastighed allerede er dokumenteret i litteraturen, er der i dette studie udviklet en ny tilgang hvor brugen af GCP'er undgås.

Det ortometriske vandniveau kan bestemmes ved hjælp af UAVs med et radar- og et GNSS (Global Navigation Satellite system). Ligesom i satellit højdemåling måler GNSS-modtageren højden over middel havniveau, medens radaren måler afstanden til vandoverfladen. Det ortopometriske vandniveau beregnes derefter ved at trække afstanden målt af radaren fra den GNSS-

afledte højde. Imidlertid har UAVs i sammenligning med satellitter flere fordele: høj rumlig opløsning, mulighed for gentagne overflyvninger, og en god genkendelse af overfladevandet. Der er dog også en del begrænsninger: vibrationer og begrænset størrelse, vægt og elektrisk effekt til sensorerne. I afhandlingen præsenteres de første studier af UAV-højdemåling omfattende bestemmelse af ortometrisk vandniveau (højden af vandoverfladen over middel havniveau) i floder og søer og i de unikke ferskvandshuller og laguner på Yucatan-halvøen. Teknikken gav mulighed for at opnå en nøjagtighed på 5-7 cm. Denne nøjagtighed er højere end opnåelig med anden luftbåren radar- eller satellitbåren LIDAR-højdemåling.

Vanddybder blev målt med en fast monteret, UAV-kontrolleret sonar. Bundniveauerne kan så estimeres ved subtraktion af vanddybden fra vandstanden. Den anvendte teknologi har til formål at kombinere den store rumlige og tidslige skala af remote sensing med nøjagtigheden af stedbundne målinger. En nøjagtighed på ca. 2.1% af den aktuelle dybde blev opnået med det udviklede system op til en potentiel vanddybde på 80 m. Remote sensing-teknik (som fx LIDAR, undervands-fotogrammetri og spektraldybde-signaturen af multi-spektral visualisering) kan kun måle vanddybder op til nogle få meter, hvorimod den her udviklede teknik har en dybdespænd og en anvendelighed, der langt overgår andre remote sensing teknikker. Sammenlignet med bemandede eller ubemandede både udstyret med ekkolod kan den UAV-bårne teknik også opmåle ikke-navigable floder og passere hindringer i flodløbet. Kombinationen af et autopilot-system og computer-baseret udsyn længere end den menneskelige synsvidde sikrer muligheden for at opnå hyper-spatiale observationer af vanddybder, uden at observatøren behøver adgang til det pågældende område.

Overfladehastigheden kan bestemmes med UAVs ved at benytte billed-kryds-korrelation. UAV-bårne vandhastighedsobservationer kan herved opnås uden de praktiske vanskeligheder af traditionelle metoder. Sædvanlige hastighedsmålinger er ofte intrusive (fx flow-målere) eller forudsætter måling fra en bådudstyret med dyre akustiske Doppler strømprofil-målere (ADCP'er). Derfor har observationer af vandhastigheden traditionelt været udfordrende, specielt i vanskeligt tilgængelige områder. Modsætningsvis giver UAV-baseret PIV (partikel–billed-hastighedsmåling) mulighed for at bestemme vandhastigheden over store områder for lave omkostninger. Et to-dimensionalt hastighedsfelt kan beregnes ved at analysere UAV-bårne video-billeder ved hjælp af stor-skala PIV-teknik. Denne teknik er velkendt på mikro-skala niveau, men stor-skala anvendelse indebærer adskillige

vanskeligheder. Det er fx ikke muligt at benytte laser-lys til at illuminere vandoverfladen. Indledende studier har vist, at teknikken kan anvendes til bestemmelse af vandhastigheder i floder. Det kræver imidlertid, at vandoverfladen tilføres partikler, da naturlige tracere i form af erosionsmateriale, bobler, eller skum normalt ikke forekommer. Ydermere er video-stabilisering essentiel for at fjerne effekterne af drone-vibrationerne. En innovative metode blev anvendt til at konvertere billed-enheder (pixels) til metriske enheder ved udnyttelse af samtidige radarobservationer fra dronen.

Et studie har været gennemført med det formål at evaluere potentialet for at udnytte UAV-bårne målinger til kalibrering af en hydrologisk model. Modellen simulerer vandstand og vandføring i Mølleåens opland. De model-beregnede estimater af interaktionen mellem grundvand og overfladevand blev betydeligt forbedrede efter udnyttelse af de syntetiske UAV-observationer. Efter kalibrering mod UAV-bårne vanstandsobservationer blev ”sharpness” reduceret med ca. 50%, RMSE (Root Mean Square Error) med ca. 75%, og retningen af fluxen mellem grundvand og overfladevand er bedre simuleret.

Table of contents

Abbreviations

ADCP	Acoustic Doppler Current Profiler
BVLOS	Beyond The Visual Line-Of-Sight
CLDS	Camera-based Laser Distance Sensor
DEM	Digital Elevation Model
GCPs	Ground Control Points
GLAS	ICESat Geoscience Laser Altimeter System
GNSS	Global Navigation Satellite System
GPS	Global Positioning System
GUI	Graphical User Interface
IMU	Inertial Measurement Unit
IHO	International Hydrographic Organization
InSAR	Interferometric Synthetic Aperture Radar
LSPIV	Large Scale Particle Image Velocimetry
mamsl	meters above mean sea level
NIR	Near Infrared
PPK	Post Processing Kinematic
PPP	Precise Point Positioning
RGB	Red Green Blue
RMSE	Root Mean Square Error
RTK	Real Time Kinematic
SAR	Synthetic Aperture Radar
SfM	Structure from Motion
SRTM	Shuttle Radar Topography Mission
SBC	Single Board Computer
SWOT	Surface Water and Ocean Topography
THU	Total Horizontal Uncertainty
TVU	Total Vertical Uncertainty
UAV	Unmanned Aerial (or Airborne) Vehicle
VTOL	Vertical Take-Off and Landing

Variables

A	area of cross section of flow
C	Chézy coefficient
CV	coefficient of variation
F	focal length
g	gravity acceleration
h	orthometric water level
ha	head loss due to acceleration
hf	head loss due to friction
HFOV	height of field of view (metric unit)
Hsens	sensor height
n_{pix_h}	number of pixels in the vertical (height) direction of the camera sensor
n_{pix_w}	number of pixels in the horizontal (width) direction of the camera sensor
OD	object distance (distance between camera lens and target)
ptdx	pixel to distance conversion in m/pix in the x-direction
ptdy	pixel to distance conversion in m/pix in the y-direction
Q	discharge though channel
S_0	bottom channel slope
Sf	friction slope
t	time
V	velocity
WFOV	width of field of view (metric unit)
Wsens	sensor width (metric unit)
x	river longitudinal coordinate
y	depth of flow
σ	standard deviation

1 Introduction

1.1 Background and motivation

The planet's water resources are very unevenly distributed, both temporally and spatially. Indeed, 97.5% of the total amount of water is saltwater and only 2.5% is freshwater. Furthermore, most freshwater exists in the form of snow, ice, groundwater and soil moisture, with only 0.3% in liquid form on the surface. Of this limited liquid surface fresh water, 87% is contained in lakes, 11% in swamps, and only 2% in rivers. Nonetheless, freshwater in lakes and rivers is the most accessible to human consumption and is essential for continental ecosystems, but is also responsible for catastrophic flood events. Given the necessity to predict dangerous hydrological events and limit water scarcity, observations of the temporal and spatial variability of surface water are essential. These hydraulic variables include elevation of the water surface above sea level, water depth (bathymetry) and water speed. Unfortunately, our knowledge of these variables is limited (Alsdorf et al., 2007). Thus, our research question is: “Can we retrieve hydraulic observations of inland surface water bodies, whenever and wherever it is required, with (i) high accuracy, (ii) high spatial resolution and (iii) at a reasonable cost?”

Unmanned aerial vehicles (UAVs), commonly known as drones, may represent the last frontier in geophysical monitoring and an innovative upgrade to the toolbox of surveyors, including hydrologists. UAVs have the potential to reduce operational costs in environmental monitoring, and can also be used for remotely sensing hydraulic variables in large areas inaccessible to operators (Tauro et al., 2015a). Furthermore, they can be used to acquire real-time hydrological data: this may be the case of extreme hydro-climatic events such as floods or droughts. In the last years, research has been undertaken to combine lightweight and low-cost sensors with sophisticated computer vision, robotics, advanced Inertial Measurement Unit (IMU) and Global Navigation Satellite System (GNSS) sensors (Colomina and Molina, 2014). Improved mission safety, autopilot systems, and reduced operational costs have ensured the repeatability of the flight missions (Watts et al., 2012) .

Thus, UAVs are a new avenue in hydrologic research and can overcome the limits of both ground-based and spaceborne hydraulic observations.

Ground-based observations suffer from insufficient monitoring networks, time gaps in records, a decreasing number of gauging stations, chronic underfunding, differences in data processing and quality control algorithms, and conflicts in data policies, which rarely support open access data (Calmant and Seyler, 2006).

Spaceborne hydraulic observations suffer from low accuracy, and coarse spatial and temporal resolution (Schumann and Domeneghetti, 2016). Indeed spaceborne instruments have a spatial resolution that is often insufficient to monitor small continental water bodies and a temporal resolution inadequate to observe rapid changes or extreme events. Furthermore, the tracking of rivers is suboptimal for most of hydrological applications due to the satellite-specific orbit patterns.

Compared to manned aircraft, UAVs offer several advantages, consisting of (i) low cost of operations, (ii) reduced time needed to plan a flight (iii) simplified landing and taking-off manoeuvres. Furthermore, the reduced flight altitude generally ensures a (iv) better spatial resolution and a (v) higher accuracy compared to manned airplanes or helicopters.

However, current UAV limitations include: (a) limited flight time, (b) low weight, size, and electric power available for the payload (c) safety and legal concerns.

1.2 Research objectives

This PhD thesis aims to demonstrate UAV-borne observations of water level, bathymetry, and surface water speed. This thesis shows that:

1. Water level (paper I) and bathymetry (paper III) can be retrieved with UAVs.
2. UAV-water level measurements can be used to calibrate river hydrological models (paper II)
3. Bathymetry and water level observations can be retrieved with UAVs in the worldwide unique cenotes and sinkholes of the Yucatan peninsula (paper IV).

4. Surface water speed can be measured with UAVs (literature review and preliminary study to confirm that surface velocity can be retrieved from UAVs)

1.3 Thesis structure

This thesis presents the methodologies and the results described in the four scientific papers. First, a chapter introduces state-of-the-art in-situ and remote sensing techniques to retrieve hydraulic observations of i) water level, ii) depth, and iii) speed.

Subsequently, the materials and methods section describes our platforms, sensors, and techniques to obtain UAV-borne hydraulic observations. This section also discusses the possibility to inform hydrological models with these new observational datatypes.

The results and discussion sections highlight the achievements of the different papers and evaluate the potential of the UAV-borne observations compared to other remote sensing techniques. Furthermore, they show the potential of UAV-borne observations for calibrating a hydrological model and improving its estimates.

In conclusion, perspectives of UAV-borne sensing in hydrology are discussed based on the research findings.

2 Progress and status of remote sensing in hydrological science

2.1 Short overview of environmental monitoring with UAVs

UAVs fill the gap between satellites and aircraft when a low-cost and an easy-to-operate monitoring platform is required for relatively long-term observation of an area (Klemas, 2015). In the last decade, UAVs have enriched the field of geophysical remote sensing with observational datasets that excel on spatial resolution and accuracy. Nowadays UAVs are commonly used in mapping vegetation cover and health, especially agricultural crops.

Berni et al. (2009) were among the scientific pioneers using UAV-borne multispectral and thermal images to estimate vegetation indices and crop water stress detection. UAV-borne observations have been used to estimate hydrological variables such as evaporation and evapotranspiration, by informing energy balance models with UAV-borne thermal data of soil and vegetation (e.g. Hoffmann et al., 2016).

UAV-borne cameras can remotely detect aquatic vegetation, both non-submerged (Husson et al., 2016) and submerged (Flynn and Chapra, 2014). UAVs have also been applied in coastal monitoring (Klemas, 2015). For instance Vousdoukas et al. (2011) have used small UAVs to provide information on the nearshore, including sand bar morphology, the locations of rip channels, and the dimensions of surf/swash zones.

However, only a limited number of studies in the published literature explored the potential of UAVs for retrieving hydraulic variables, such as water speed, level, and depth. In the next chapter, in order to explore the benefits of UAV-borne sensing in this field, we will describe the limitations of retrieving these hydraulic variables with spaceborne, manned airborne or ground-based platforms.

2.2 Water level

The comprehensive review by Alsdorf et al. (2007) highlights the importance of temporal and spatial variations of water levels and water volumes stored in rivers, lakes, reservoirs, floodplains, and wetlands. In this regard, water surface (**h**), temporal changes in water levels (**∂h/∂t**), water surface slope (**∂h/∂x**), and inundated area are the measurements that need to be retrieved. These are also the quantities simulated by hydrodynamic models.

2.2.1 In-situ water level measurements

Ground-based measuring stations can accurately retrieve **h** with high temporal resolution, allowing precise estimation of **∂h/∂t** when there are no gaps in the record. However, gauging stations are single point-measurements; therefore, the spatial multidimensional variability of water level and the hydraulic gradient (**∂h/∂x**) cannot be estimated from ground-based networks only. Furthermore, data from ground-based stations are generally organized on a national or regional basis. This results in different data processing, quality control, and data access policies. Several countries do not share their data or have complicated and expensive data access procedures (Durand et al., 2010). Lastly, several areas in the world are poorly sampled due to underfunding or political instabilities. In this regard, there has been a consistent fall in the number of available records since 1980 (Calmant et al., 2008).

2.2.2 Spaceborne water level measurements

Because in-situ stations do not currently provide consistent hydraulic observations with reasonably uniform spatial distribution, elevation of water surfaces has been routinely monitored by spaceborne and airborne platforms in the last 20-30 years. Despite being primarily designed and optimized for ocean water heights or polar ice surveys, satellite altimetry missions have been used to monitor terrestrial water bodies. Some pioneering studies (e.g. Birkett, 1998; Brooks, 1982; Koblinsky and Clarke, 1993; Morris and Gill, 1994a, 1994b) analysed the potential of altimetry data for estimating water elevation in large lakes, reservoirs and wide rivers. Their focus was on the first altimetry missions: Seasat, Topex/Poseidon, and GeoSat.

In the past two decades, several altimetry missions have been launched, as shown in Figure 1.

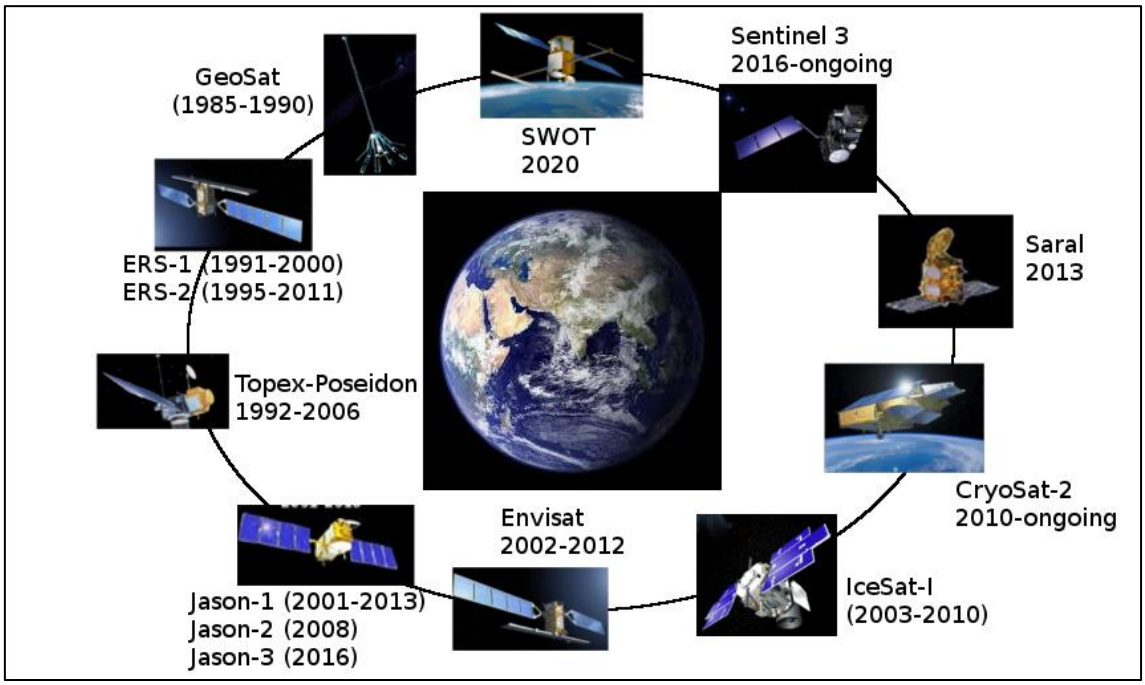

Figure 1. Graphical illustration showing some of the past, current or future satellite missions that are most commonly reported in the literature concerning water level observations of inland water bodies. Each satellite has its own orbit, different from the others.

These on-board altimetry instruments have ground footprints that are generally less than 1 km. Since the topography that surrounds a river can often "contaminate" the return echoes, water surface elevation can be retrieved only in water bodies with a size comparable or even larger than the ground footprint (O'Loughlin et al., 2016). For example, Birkett et al. (2002) showed that, although TOPEX/Poseidon has a 600 m ground footprint, water bodies need to have of width of at least 1.5 km to be accurately monitored. However, retracking algorithms can select the target based on the range and strength of the echo (Berry et al., 2005; Birkinshaw et al., 2010). In this regard, water level of medium sized rivers (width between 100 and 1000 m) can be identified by taking into account the exact location, width, and shape of the river in processing the data (Maillard et al., 2015). In this case, the obtained accuracy can be comparable to the one achieved for much larger rivers, i.e. typical error ranges from ~30 to 70 cm depending on altimetry product (Biancamaria et al., 2017; Michailovsky et al., 2012; Sulistioadi et al., 2015).

ICESat has been so far the only LIDAR satellite mission to provide elevation of water surface. The Geoscience Laser Altimeter System (GLAS) on board ICESat has a ground footprint of around 60-70 m and an along track distance between consecutive footprints of 170 m (Phan et al., 2012). A few studies have assessed the accuracy of GLAS in monitoring inland water level. Hall et al. (2012) found a mean absolute error between gauge data of Mississippi basin and ICESat of 19 cm. Baghdadi et al. (2011) found a similar accuracy of 15 cm for Lake Léman, however the root mean square error in French rivers was estimated to be ca. 1.15 m. Indeed, when the width of the water body is similar to the ground footprint (~70 m), multiple returns from the land surface contaminate the signal.

Therefore, radar and laser altimetry missions can provide measurements of the water level (**h**) with accuracy of few decimetres and low spatial resolution. However, the measurements of temporal $\partial\mathbf{h}/\partial\mathbf{t}$ and spatial $\partial\mathbf{h}/\partial\mathbf{x}$ variability are still a major challenge.

$\partial\mathbf{h}/\partial\mathbf{t}$ can be computed by observing changes in observed water level when the satellite revisits the same water body. However, repeat cycles for satellite altimetry missions are typically several days to weeks and long-repeat satellites such as CryoSat have a revisit times in excess of one year.

$\partial\mathbf{h}/\partial\mathbf{x}$ can be computed only when the orbital track is subparallel to an elongated water body. Indeed all altimeters are profiling instruments, with no imaging capability. In this regard, the Shuttle Radar Topography Mission (SRTM) is the only space shuttle mission that provided spaceborne image-based observations of water level, but only for a single snapshot in time (11 days in February 2000). Slope ($\partial\mathbf{h}/\partial\mathbf{x}$) of a river can be estimated from a SRTM-derived DEM. However the accuracy in height determination is of several meters (Kiel et al., 2006; LeFavour and Alsdorf, 2005), therefore the computed water slope is not reliable unless rivers are long enough to accommodate for measuring errors.

The new Surface Water and Ocean Topography (SWOT) mission, expected to be launched in 2021, will gather SRTM heritage. SWOT is expected to accurately measure distributed water level (**h**), $\partial\mathbf{h}/\partial\mathbf{x}$, and $\partial\mathbf{h}/\partial\mathbf{t}$ of wetlands, rivers, lakes, reservoirs (Durand et al., 2008; Neeck et al., 2012). According to NASA the mission will provide a “water mask able to resolve 100-m rivers and 1-km2 lakes, wetlands, or reservoirs. Associated with this mask there will be water level elevations with an accuracy of 10 cm and a slope accuracy of 1 cm/1 km”.

However, spaceborne remote sensing will always have to face some limitations in monitoring **h** and estimating $\partial\mathbf{h}/\partial\mathbf{x}$, $\partial\mathbf{h}/\partial\mathbf{t}$. Indeed, spaceborne satellite missions are limited by: i) a large ground footprint, which determines a low spatial resolution; ii) a suboptimal measurement accuracy for most hydrological models ii) a coarse temporal resolution and the inability to retrieve real-time observations iii) a coarse tracking of inland water bodies due to the predetermined orbit patterns. For all of these reasons, spaceborne missions cannot singularly supply all information required to guide water resource and flood hazard management.

2.2.3 Airborne water level measurements

Water level can be remotely sensed by LIDAR instruments on board manned aircrafts.

However, accurate determination of the water surface is not trivial for LIDAR instruments (Guenther, 1981). LIDAR instruments need higher energy and longer pulse for detecting water surface than for surveying land surface. Near infrared (NIR) wavelength is generally used for monitoring of water surface, indeed NIR shows low penetration below the air-water interface. Conversely, green wavelengths travel through the air-water interface up to the bottom of the water body, thus data have to be processed with waveform analysis algorithms. These algorithms allow retrieval of the two reflection peaks: the first pulse returned from the water surface and the second returned from the bottom, as shown in Figure 2.

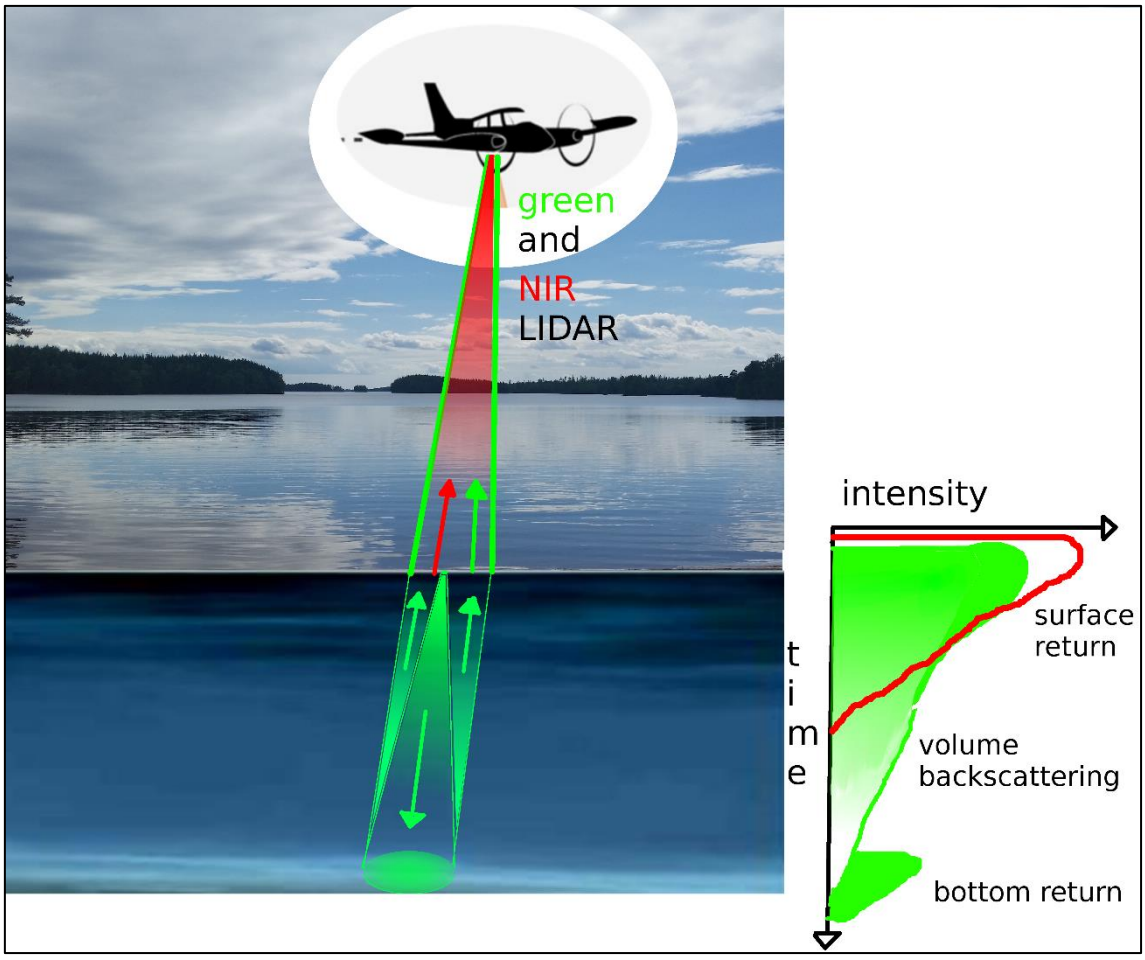

Figure 2. Airborne LIDAR with two frequencies: green and NIR. Depending on system design, the NIR beam may be collimated with the green beam, or it may be broader and constrained at nadir. Green wavelength has two major return echoes: from the bottom and from the water surface. The volume backscatter return derives from particulate suspended in the water column under the air-water interface. Conversely, NIR wavelength penetrates very little: it can be used for detection of the water surface.

Albeit airborne LIDAR sensors have a reported technical accuracy around 10-20 cm, few scientific studies report the accuracies of airborne LIDARs in monitoring rivers. Indeed, the accuracy depends on surrounding topography (e.g. geometry and size of the water surfaces, relief, and aquatic or riparian vegetation canopy). Hopkinson et al. (2011) estimated an accuracy range from few cm to two tens of cm in the Mackenzie Delta by comparing LIDAR data with hydrometric gauges. Schumann et al. (2008) compared LIDAR-derived observations with the water level computed by a flood inundation model in a floodplain area of Alzette River, Luxembourg City. The results

show that LIDAR-derived water stages exhibit a RMSE value of around 0.35 m.

Besides these accuracy limits, the high cost of airborne LiDAR surveys is the main constraint and causes two main limitations: i) scarce spatial coverage ii) temporal coverage limited to specific time intervals, which do not often correspond to periods of hydrological interests.

2.2.4 UAV-borne water level measurements

In this regard, the advantage of using UAVs is to overcome the described limitations of satellite and ground-based observations, retrieving observations at a limited cost during intervals of hydrological interest in specific areas, which may be inaccessible to human operators.

However, the possibility to retrieve accurate, highly resolved water level from UAVs has not been documented so far in the literature. A few scientific studies described photogrammetric techniques to obtain Digital Elevation Models (DEMs) of the water surface of rivers. The photogrammetric Structure from Motion (SfM) technique is a well-known method to reconstruct DEMs from UAV imagery, but its success in monitoring water level strongly depends on: i) river shape, ii) absence of vegetation overhanging the river body and iii) water turbidity that prevents light from penetrating below the surface and avoids acquisition of submerged topography. Furthermore, photogrammetry generally requires ground control points (GCPs). Niedzielski et al. (2016) adopted a different approach to geo-rectify UAV-borne images, omitting the use of GCPs. In this case, a previous airborne LIDAR survey was used to obtain a spatial fix and correct for errors during orthomosaicking. The extent of the water surface was observed and river stages were simply classified between low, normal, and high-flow situations.

2.3 Water depth

Knowledge of bathymetry is critical for estimating water volume and discharge; furthermore, it is essential to study geomorphology (Lejot et al., 2007) and river processes, including sediment transport budgets (Irish, 1997).

2.3.1 In-situ measurements of water depth

Accurate bathymetric surveys can be conducted by using vertical single-beam echo-sounders, while expensive multi-beam echo-sounders can be used to improve coverage of the measurement and speed of surveys. These ultrasonic sensors (sonars) need to be in contact with the water surface, therefore are generally dragged by boats or aquatic drones (e.g. Giordano et al., 2015).

2.3.2 Spaceborne measurements of water depth

Unfortunately, no spaceborne active remote sensing method can penetrate water to the necessary depths. However, passive optical imagery from high resolution satellites (Quickboard, IKONOS, Worldview-2) and medium resolution satellites (e.g. Landsat) has been used to estimate bathymetry by observing the relations between spectral signature and depth (Hamylton et al., 2015; Lee et al., 2011; Liceaga-Correa and Euan-Avila, 2002; Lyons et al., 2011; Stumpf et al., 2003). Water spectral signature can be used as a proxy for estimating bathymetry only when water is very clear and shallow (water depth 1-1.5 times the Secchi depth), the sediment is comparatively homogeneous, and the atmosphere is favourable (Lyzenga, 1981; Lyzenga et al., 2006).

2.3.3 Airborne measurements of water depth

Based on many years of operations, airborne LIDAR has proven to be an accurate method for surveying in shallow water and coastlines. For an eye-safe airborne LIDAR, the maximum depth that can be surveyed is expected to be around 50 meters in offshore “crystal” clear waters. However, penetration depth is generally limited to depths between 2 and 3 times the Secchi depth, which results in few decimetres-meters in inland water bodies (Guenther, 2001). Beside water clarity, also bottom reflectivity, waviness and solar

background play a key role (Banic, 1998). Therefore, accuracy of LIDAR depends on the deployed optics, on the atmospheric conditions, on water turbidity and waviness. Post-processing of the results is generally complex and requires correction for factors such as refraction index and removal of volume backscattering effects (as shown in Figure 2). Perry (1999) found an accuracy of 0.24 meters at 95% confidence interval for 84500 points at depths ranging from 6-30 meters, but in sea areas, where water is very clear.

Hilldale and Raff (2008) evaluated the accuracy for 220 river kilometres in the Yakima and Trinity River Basins in the USA. The accuracy was found correlated with the slope of the river bed, with an accuracy of around 0.05 m for slope of less than 10% and accuracy of around 0.5 m for slope more than 20%. High relief features strongly affect accuracy, since the laser beam has a footprint of around 2 m and only process the first return pulse. Furthermore, the penetration of LIDAR pulses is limited to few meters in rivers because of water clarity issues.

2.3.4 UAV-borne measurements of water depth

A novel UAV-borne topo-bathymetric laser profiler, Bathymetric Depth Finder BDF-1, has recently entered the market in 2016. This profiler LIDAR can retrieve measurements only up to 1-1.5 time the Secchi depth, thus it is designed for gravel-bed shallow water. Mandlburger et al. (2016) presented this system after having tested it in a pre-alpine river. The river bottom heights differed from the reference measurements by a calculated bias of about 10 cm in the riverbed and 8 cm at the bank with standard deviations of 13 cm and 17 cm, respectively. The sensor is an absolute novelty in the UAV-remote sensing field; however, its disadvantages are the high cost and the weight of ca. 5.3 kg. Because of this weight, only UAVs with a payload capability greater than 5 kg can lift it: a UAV named BathyCopter was specifically developed by the manufacturer for this purpose.

UAV-borne multi-spectral, hyper-spectral and optical cameras have been used to estimate water depth. The radiances measured at different wavelengths from shallow water is a proxy estimate of depth, as with satellite-derived imagery (Lyzenga et al., 2006). To be successful, passive remote sensing of water depth needs 1) clear water (maximum depth nearly equal to the Secchi depth) ii) calm flat water surface to avoid ripples iii) unobstructed view of the river. Several scientific studies have assessed the accuracy of UAV-borne passive remote sensing of water depth in gravel bed clear water.

Flener et al. (2013) applied Lyzenga's (1981) linear transform model. They estimated a RMSE between 8 and 10 cm, but the error was doubled when computing the ellipsoidal height of the river bed because of errors in water surface detection. Tamminga et al. (2014) firstly obtained a DEM model retrieved by ortho-mosaicking UAV-borne of Elbow river, Canada. Then, in order to perform reliable though-water photogrammetry, they corrected the DEM by using two methods: i) corrective factor for water refraction index ii) an empirically calibrated depth estimate based on pixel colour values. Both methods showed weaknesses and strengths, with a RMSE of around 12-13 cm when compared to checkpoint elevations.

2.4 Surface velocity

Surface velocity data are essential to study flow pattern, erosion patterns (Kantoush and Schleiss, 2009) and estimate discharge.

2.4.1 In-situ measurements of surface velocity

Intrusive measurements with flow meters require immersion of the flow meter in different points of a river section to retrieve horizontal and vertical profiles (Tazioli, 2011). Only Acoustic Doppler Current Profiler (ADCP) can retrieve full vertical and horizontal water velocity profiles (Yorke and Oberg, 2002). ADCPs need to be in contact with the water surface, generally require expert operators, are time-consuming and rather expensive.

Because of these constraints, many scientists have worked on methods to measure surface speed, with more efficient, non-invasive, techniques. Large Scale Particle Image Velocimetry (LSPIV) is an optical technique that allows characterization of surface currents based on digital images or videos of the water surface. Several studies assessed the potential of LSPIV in monitoring surface speed of inland water bodies from static locations above or on one side of a river (Creutin et al., 2003; Hauet et al., 2008; Jodeau et al., 2008).

2.4.2 Spaceborne measurements of surface velocity

So far, no spaceborne sensor has been successful in measuring water speed. Surface velocity in rivers could be theoretically measured from satellites with Doppler LIDAR or radar. For instance spaceborne satellite LIDARs could potentially retrieve surface velocity, or at least one spatial component, with a potential accuracy on the order of 0.1 m/s (Bjerklie et al., 2005).

A few studies tried to obtain reliable observations of surface water speed with interferometric processing of an along-track synthetic aperture radar data. For instance, Romeiser et al. (2007) demonstrated that they could identify surface current fields in Elbe river (Germany) with the along-track distance between the two SAR antennas of the SRTM. However, the short time lag between the two InSAR images of the SRTM resulted in low sensitivity to small velocity variations and low signal-to-noise ratio of phase images. For this reason, topographic features could contaminate the signal and images were averaged over many pixels for accurate velocity estimates.

2.4.3 Airborne measurements of surface velocity

Airborne Doppler LIDAR and interferometric processing of two SAR antennas are promising techniques to retrieve surface water current. However, their use is mainly documented for ocean environments and few studies analysed the use of interferometric SAR for river environments (e.g. Bjerklie et al., 2005).

2.4.4 UAV-borne measurements of surface velocity

UAV application of LSPIV has a short but successful history in monitoring surface water speed (Detert and Weitbrecht, 2015; Tauro et al., 2016b, 2015a).

A fascinating new contribution was presented at EGU 2015 regarding a miniaturized Doppler radar sensor, operating at 24 GHz, to measure surface water speed (Virili et al., 2015).

3 Materials and methods

In this section, the importance of water level, speed, and velocity observations in hydrodynamic river modelling is analysed. Then, the UAV platforms and payloads, which were used to retrieve hydrodynamic observations, are described. The last part of this section shows how UAV-borne observations are processed in order to inform a hydrological model.

3.1 Hydrodynamic models

Navier-Stokes equations are the basis of computational hydrodynamic models. When the horizontal length scale is much greater than the vertical length scale, Navier-Stokes equations are simplified into the shallow water equations. Shallow water equations can be further simplified into the commonly used 1D Saint-Venant equations assuming that: i) Flow is one-dimensional; ii) boundary friction can be accounted through simple resistance laws analogous to steady flow; iii) small bed slopes (Cheviron and Moussa, 2016). The 1D Saint-Venant equations are shown in Table 1 in their non-conservation form:

(1) describes the conservation of mass and (2) describes the conservation of momentum.

Table 1. The 1D Saint-Venant equations. Symbols are explained in Figure 3 and in the symbol list at the beginning of the thesis.

$$y\frac{\partial V}{\partial x} = -V\frac{\partial y}{\partial x} - \frac{\partial y}{\partial t} \quad (1)$$

$$\frac{\partial V}{\partial t} + V\frac{\partial V}{\partial x} = g(S_0 - Sf) - g\frac{\partial y}{\partial x} \quad (2)$$

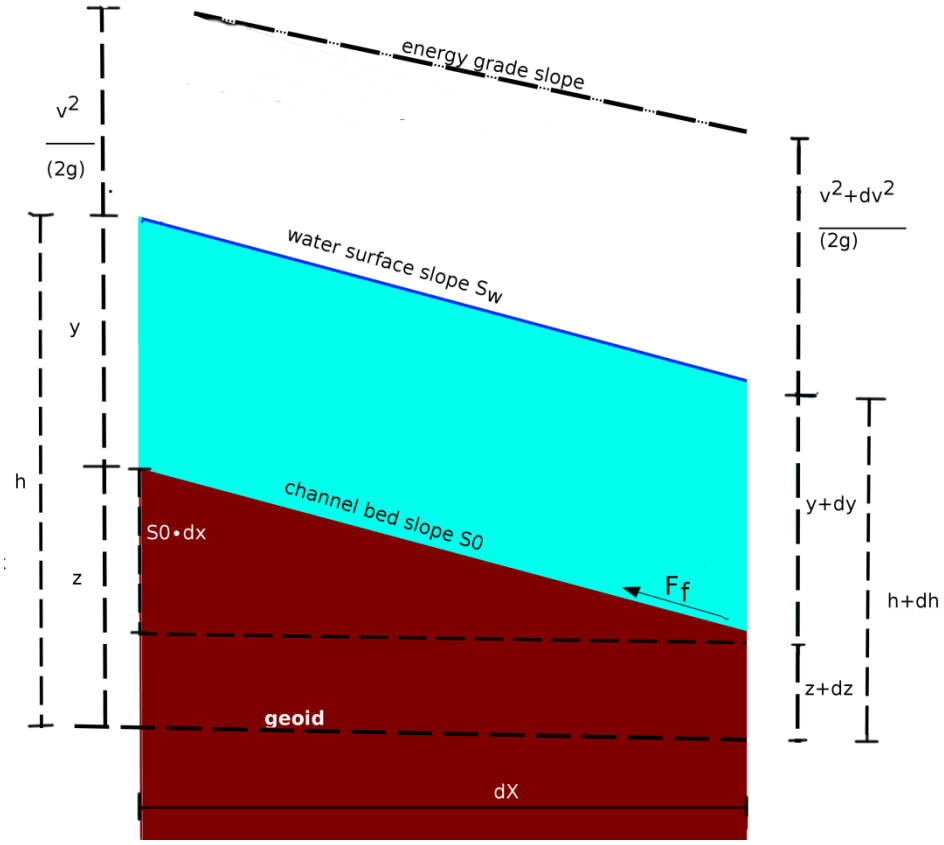

Figure 3. Simplified reproduction of the sketch shown in Chow (1959). It shows the main variables appearing in the 1D Saint-Venant equations. F_f is the force due friction. It can be computed as $F_f = \rho \cdot g \cdot A \cdot S_f \cdot dx$, in which ρ is density, g is gravity, A is cross section areas, S_f is the friction slope, and dx is the spatial increment.

Figure 4 shows that UAVs can provide the observations needed to solve these two equations. Indeed, during this PhD, UAVs have been be employed to measure the bed slope S_0 and the water depth (y), including its spatial $\frac{\partial y}{\partial x}$ and temporal $\frac{\partial y}{\partial t}$ derivatives.

Only the friction slope Sf is not directly observable. Sf is generally expressed as $\frac{V^2}{R \cdot C^2}$, in which V is velocity, R is hydraulic radius and C is Chézy coefficient. However, the Chézy coefficient (or the derived Manning coefficient) can be obtained by model calibration against UAV observations (paper II).

UAV-borne surface velocity measurements can also be used to validate the output of the river hydrodynamic models in terms of the $\frac{\partial V}{\partial x}$ and $\frac{\partial V}{\partial t}$. To estimate the spatial and temporal derivative of velocity, surface water velocity needs to be converted into mean velocity in the vertical water column. The

theoretical “mean to surface velocity” ratio of 0.85 (Rantz, 1982) is valid for a wide range of depths, low to moderate bottom roughness values and mild slopes. This 0.85 coefficient is based on the assumption that water velocity increases vertically with the logarithm of the distance from the river bottom.

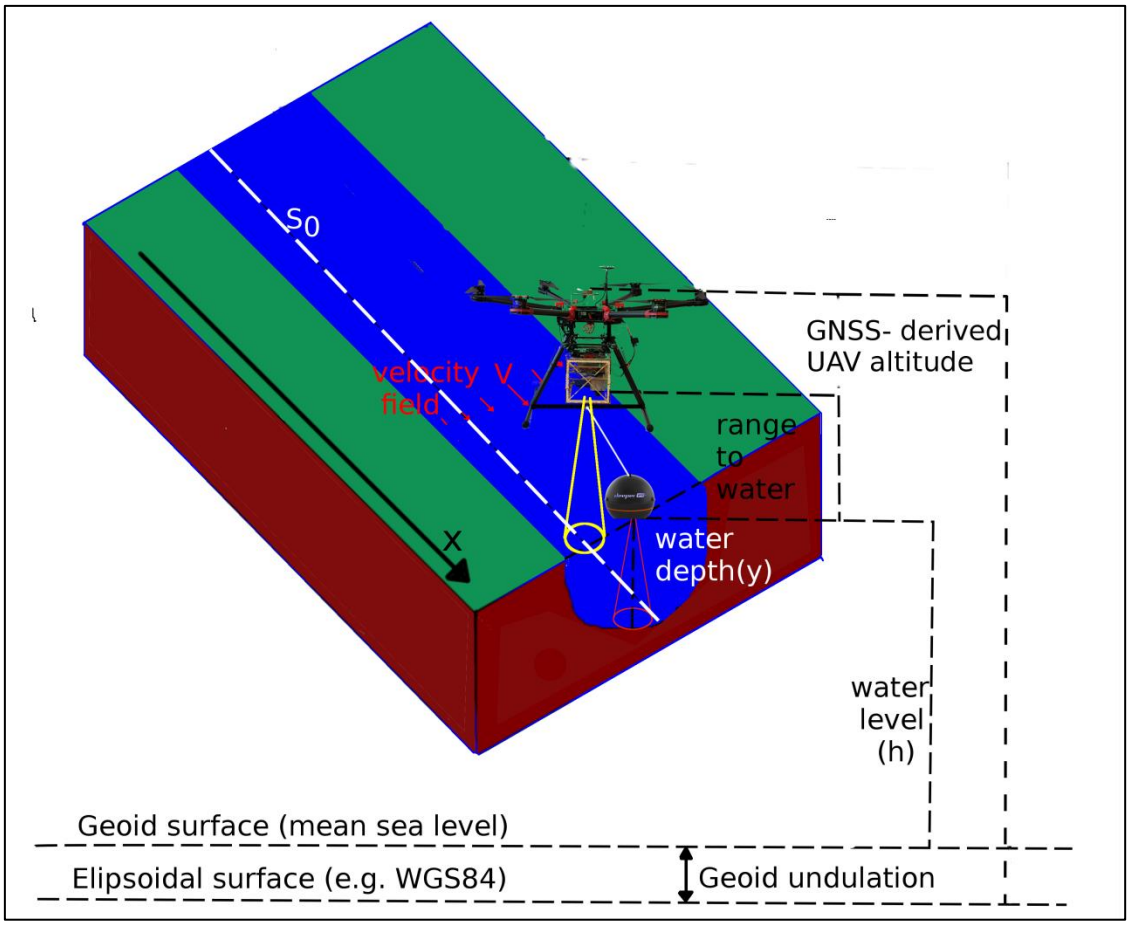

Figure 4. UAVs can provide observations to inform the Saint-Venant equations.

Open-channel flow models (e.g. HEC-RAS, MIKE 11, SWMM5, InfoWorks, Flood Modeller) implement the 1D Saint-Venant equations shown in Table 1. These 1D open-channel hydrodynamic models require as basic input: i) geometry of some river cross sections ii) river shape and length iii) geometry and properties of the river structures (dams, bridges, culverts, weirs..) iv) roughness coefficients, and v) boundary and initial conditions. They simulate water level, depth and discharge time series at each computational node.

Our UAV-borne bathymetric sensors can observe bathymetry and UAV imagery can provide observations of river shape, river length, and river struc-

ture geometry. Thus, these observations can be directly used to inform open-channel models. Roughness and head loss coefficients of river structures can be obtained by model calibration using UAV-borne water level observations as calibration objective (Bandini et al., II). Similarly, velocity observations can also be used as calibration objective.

3.1.1 Two-dimensional hydrodynamic models

2D hydrodynamic models generally implement the 2D version of the Saint-Venant equations and simulate two-dimensional flow. A detailed description of the 2D flow field is generally required in floodplains, wetlands, urbanized areas, lake or estuaries, alluvial fans and downstream of leave breaks. 2D models require more time to setup and run, and require more input data, than 1D model. For instance, detailed topographic data of both the river and the flooded area are required at each grid point. The scarcity of these data is one of the main constraints for the implementation of these 2D models. However, our UAV payload for measuring bathymetry can provide detailed topographic data of the submerged area. Similarly, SfM techniques, applied to UAV images, can provide DEM of the non-submerged topography. Furthermore, UAV-borne 2D surface water velocity speed and UAV-borne water level observations, retrieved along and across the direction of the main flow, can be used as calibration objective of these 2D models.

3.1.2 Discharge estimation

Discharge is not a directly observed quantity: it is derived from depth-integrated water speed profiles and cross-sectional area. Our bathymetry measurements can retrieve the cross-sectional area and the water depth. However, discharge estimation would require depth-integrated water speed profile, while UAVs can only directly measure surface velocity. Although water surface speed is influenced by wind and river turbulence (Plant et al., 2005), 2005), surface speed can be used to estimate velocity profiles in the vertical water column by using logarithmic equations (Rantz, 1982). Another intriguing approach has been documented by Moramarco et al. (2013) in which

Chiu (1988)'s entropy model is used to estimated mean flow from maximum flow, which typically occurs in the upper portion of the flow area.

By combining cross sectional areas and mean velocity observations, discharge can be estimated by using UAV-borne observations only.

3.2 UAV platforms

The majority of the flights were conducted with rotary wing platforms (Bandini et al., I, II, III, IV). Rotary wing UAVs ensure (a) high manoeuvrability, (b) vertical take-off, (c) vertical landing, and (d) hovering capability. Conversely, fixed wing UAVs ensure (1) long flight time and distances, with (2) high stability and (3) reduced vibrations.

The main goal of the SmartUAV project, which is financing this PhD, has been to develop a hybrid UAV platform with combined fixed wing and rotary wing capabilities.

As described in Bandini et al. (IV), a VTOL (Vertical Take-Off and Landing) hybrid platform would allow for i) long flight range, ii) high manoeuvrability, iii) vertical take-off iv) vertical landing, and v) BVLOS capability.

The first test flights on this hybrid platform, which has been developed in collaboration between Sky-Watch, DTU Space and DTU Environment, have been conducted in early 2017. Although the platform development is not completed, the hybrid UAV shows a good potential for monitoring water targets due to the possibility of flying long range and hovering over the designed target for acquiring observations. However, the authorizations to conduct flights BVLOS have not been acquired yet.

Figure 5 compares the different platforms flown during the PhD.

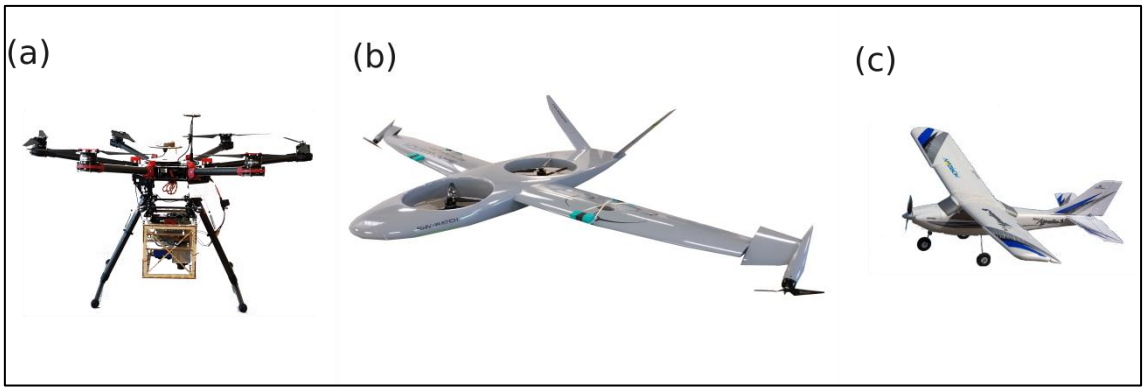

Figure 5. UAV platforms flown during the PhD. (a) multirotor rotary wing (DJI S900): maximum take-off weight 8.2 kg, maximum payload of ca. 2 kg, and a wing span of ca. 1 m. (b) Hybrid UAV with VTOL capability (SmartUAV). This platform is the largest between the shown UAVs: total weight of ca. 15 kg (maximum payload capability of only 1.5 kg) and a wing span of ca. 5 m. (c) fixed wing (Mini Apprentice S.): maximum take-off weight of ca. 735 g, with payload capability of ca. 100 g, and a wing span of ca. 1.2 m.

3.3 Payload

Three different payloads were assembled to retrieve hydraulic observations: water level, depth, and surface velocity.

The sensors in common on each payload are: i) a RGB digital camera ii) an IMU system to measure the drone angular and linear motion and iii) a GNSS system to measure vertical and horizontal geographical coordinates.

The RGB camera is a Sony DSC-RX100.

The IMU is a Xsense MTi 10-series.

The GNSS system consists of a GNSS receiver (OEM628 board) and an Antcom (3G0XX16A4-XT-1-4-Cert) dual frequency GPS and GLONASS flight antenna. To obtain cm-level accurate drone position the GNSS (GPS and GLONASS) observations are post-processed with post-processed kinematic (PPK) technique in Leica Geo Office software. This PPK technique is a carrier-phase differential GNSS method that can correct for the GNSS errors in

common between two receivers (e.g. satellite orbit errors, satellite clock errors, atmospheric errors). Only multipath errors and noise of the individual receivers cannot be corrected in differential mode since they are uncorrelated. Differential GNSS requires the availability of a base-station. A NovAtel flexpack6 receiver with a NovAtel GPS-703-GGG pinwheel triple frequency (GPS and GLONASS) antenna was used as base-station in most of the flights.

PPK technique was preferred to the Real Time Kinematic (RTK) technique to process the carrier-phase GNSS observations. Indeed PPK solution is a posteriori post-processing of the data and can use the GNSS acquisition of both the previous and the next time step to improve integer ambiguity solution and estimate solution consistency. Conversely, when RTK method is applied, only data recorded in the previous time stamps can be part of the position solution computed by the Kalman filter based algorithms.

Observations of the different sensors are synchronized and pre-processed in-flight on the microprocessor BeagleBone Black: a single board computer (SBC) running Linux Debian O/S. This SBC (commonly referred to as microprocessor) was programmed in C/C++ language in order to receive data from the hardware interface of each sensor (e.g. CAN bus interface for radar, UART for GNSS and IMU, active-low/high logic from RGB camera, etc…) and save data using unique Linux timestamps on the SBC's memory. In this way, the sensor observations can be synchronized together at the millisecond level and observations can be geotagged with drone coordinates.

3.3.1 Payload to measure water level

Bandini et al. (I) described the methodology to measure orthometric water level elevation (height of the water surface above mean sea level) with UAVs. To take these measurements, two sensors are needed: a ranging sensor and a GNSS system. The ranging sensor measures the range between the UAV and the water surface, while the GNSS system measures the GNSS altitude above the reference WGS84 ellipsoid (convertible into altitude above geoid). Water level is then derived by subtracting the observations of the ranging sensor from the altitude retrieved by the GNSS receiver (as shown in Figure 4).

Different ranging sensors were tested and evaluated in Bandini et al. (I).

These ranging sensors include: i) 77 GHz radar (Continental RS 30X) ii) 42 kHz sonar (MaxBotix MB7386) and iii) camera-based laser distance sensor

(CLDS) prototype developed during the PhD project. The payload is shown in Figure 6. Accuracy, beam divergence, precision, maximum range capability of each of the sensor were evaluated with static and airborne tests over rivers and lakes.

After these evaluation tests, only the radar system was employed to retrieve water level observations in Bandini et al. (II, III, IV).

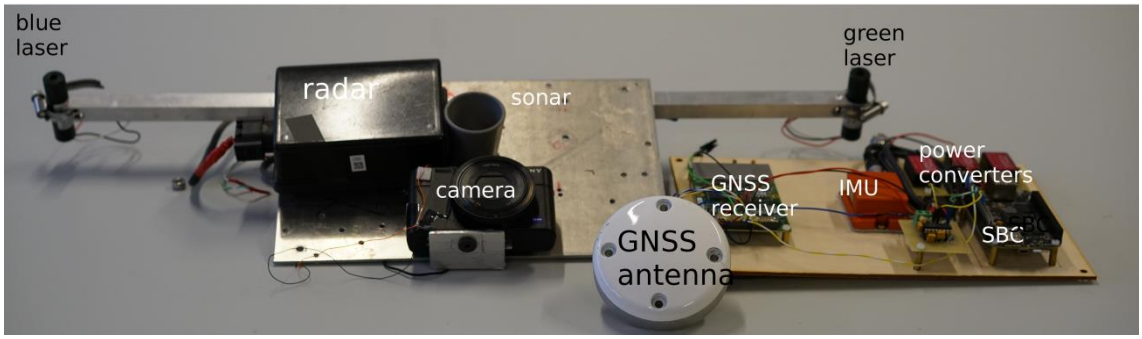

Figure 6. Picture modified from Bandini et al. (I). The water level ranging payload includes a GNSS receiver, IMU, radar, 42 kHz sonar, CLDS (consisting of two laser pointers and an optical RGB digital camera). In addition, power conversion units and a SBC are included.

3.3.2 Payload to measure water depth (and bathymetry)

A bathymetric lightweight 290 kHz and 90 kHz dual frequency sonar, Deeper UAB, is employed to measure water depth. Because of the different acoustic refraction index of water and air (different sound speed), bathymetry sonars always need to be positioned in contact with the water surface. Thus, the bathymetric sonar cannot be located on board the UAV, but is tethered and dragged by the drone on the water surface. The accuracy (ca. 2.1% of the actual depth) and maximum water depth capability (potentially up to 80 m, tested up to 35 m) are reported in Bandini et al. (III). Bandini et al. (III) also describes the payload system and the set of equations to measure accurate geographic coordinates of the sonar.

Bathymetry observations (orthometric bottom elevation) can be directly derived by subtracting water depth from water level observations.

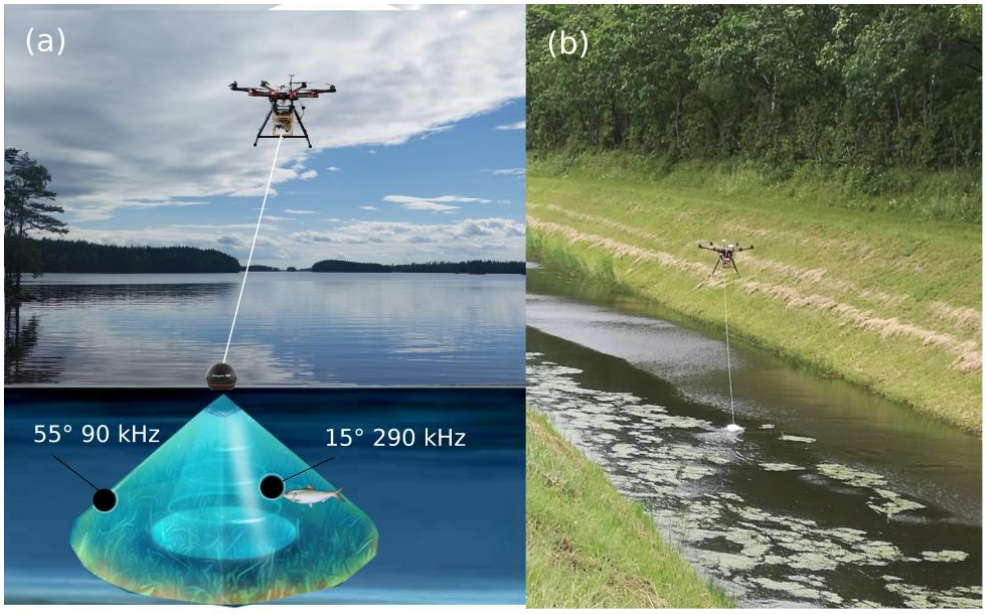

Figure 7. UAV tethered sonar to measure bathymetry. (a) sonar measuring beam, two different frequencies with their respective beam divergence. Modified figure from Bandini et al (IV) (b) picture of the UAV flying above a Danish river.

3.3.3 Payload to measure surface flow speed

During Holm and Goosmann's (2016) special course project, we developed a payload to measure surface water speed with LSPIV technique (Hauet et al., 2008; Jodeau et al., 2008). The LSPIV is a non-contact technique that provides velocity measurement by quantifying the movement of small and light particles moving across a river transect. The particles (tracers) are expected to accurately follow the underlying flow and be uniformly distributed in the area to be measured (Muste et al., 2014). The difference in the tracers position between consecutive frames (displacement vector) is computed with autocorrelation or cross-correlation techniques (Raffel et al., 2007).

UAV or airborne LSPIV generally require the usage of tracers (Fujita and Hino, 2003), either natural (bubbles, debris, foam) or artificial seeding (e.g. woodchips). An artificial tracer is commonly used in UAV-borne LSPIV implementation. For example according to Detert and Weitbrecht (2015) particles used a as tracers "should have a sufficient floating behaviour, significant colour contrast, a passive respond to the flow, the possibility of a simple mass production at adequate dimensions, and no effect on the water quality". However, Fujita and Kunita (2011) demonstrated that an oblique-scanning helicopter-mounted camera can identify the movement of the water surface by examining water ripples generated by turbulence or differences in colour

caused by variations in suspended sediment concentration, without the need for artificial tracers.

UAV-borne LSPIV is affected by drone movement and vibrations (Tauro et al., 2015a), thus requires extensive and time-consuming image processing algorithms to stabilize videos (Fujita and Kunita, 2011).

Ortho-rectification of the image is performed to convert from image units (pixels) into real-word distance unit. Generally at least 4 GCPs are acquired for image calibration and ortho-rectification, thus the area must be accessible to human operators (Kim et al., 2008; Tauro et al., 2015a). In this regard, Tauro et al. (2016a, 2014) experimented with using laser pointers on permanent gauges (not UAVs) to estimate true distances in the image domain and avoid the usage of GCPs. These lasers are positioned at a known distance between each other and pointed towards the water surface. Thus, the distance between the two laser dots on the image of the water surface can be used to convert pixel units into metric units.

Our water velocity ranging payload consists of a video-camera (the RGB camera Sony DSC-RX100) and the 77 GHz radar (Continental RS 30X). The camera is mounted on the UAV without any gimbal. It retrieves a video of the water surface at nadir angle. Video sequences are generally retrieved for 1-2 minutes with the drone hovering at a fixed position over the river. Then videos are stabilized to remove high frequency vibrations. This procedure requires 1-2 reference stable points (e.g. rocks, soil) identified in the riverbanks.

Then LSPIV analysis is performed with the Matlab toolbox PIVlab (Thielicke and Stamhuis, 2014). The 2D velocity vectors are initially computed in pixel units. Conversion from pixel units into metric units is performed with an innovative approach that does not require GCPs, but consists of the following steps i) lens distortion is removed using commercial software PTLENS (http://epaperpress.com/ptlens/index.html), ii) pixel distance is converted into metric units with the equations shown in Table 2, in which the range to the water surface measured by the radar (OD) is required as input.

Table 2, equations to convert from pixel distance into metric units. Symbols are explained in the symbol list at the beginning of this document and in Figure 8.

$$WFOV = Wsens \cdot \frac{OD}{F} \quad (3)$$

$$HFOV = Hsens \cdot \frac{OD}{F} \quad (4)$$

$$ptdx = \frac{WFOV}{n_{pix\_w}} \quad (5)$$

$$ptdy = \frac{HFOV}{n_{pix\_h}} \quad (6)$$

Equations in Table 2 are implemented to convert from the width and height (Hsens and Wsens) parameters of the sensor into the width and height of the image field of view (WFOV and HFOV). This is done through the relationship between the range to water surface (OD) and the focal length (F). These variables are shown in Figure 8.

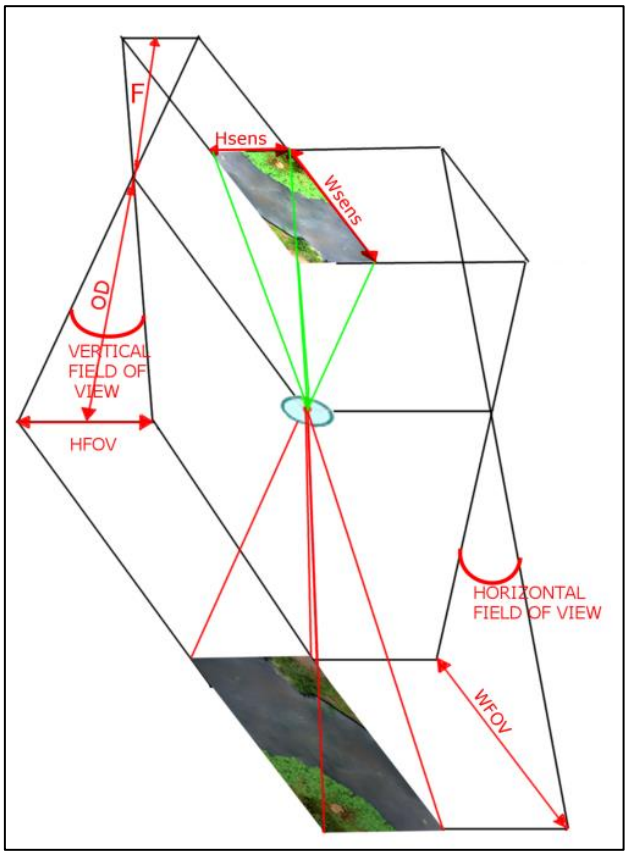

Figure 8. Representation of a camera field of view.

Subsequently, dividing WFOV and HFOV by the number of horizontal and vertical pixels, the vertical and horizontal pixel resolution, ptdx and ptdy, are computed. The variables ptdx and ptdy are computed in "metric units per pixel" and allow converting from image distances into real distances.

3.4 Processing of UAV-borne measurements

The flowchart shows the processing steps required to acquire UAV-borne observations and use them to calibrate an open-channel flow model (e.g. Mike 11).

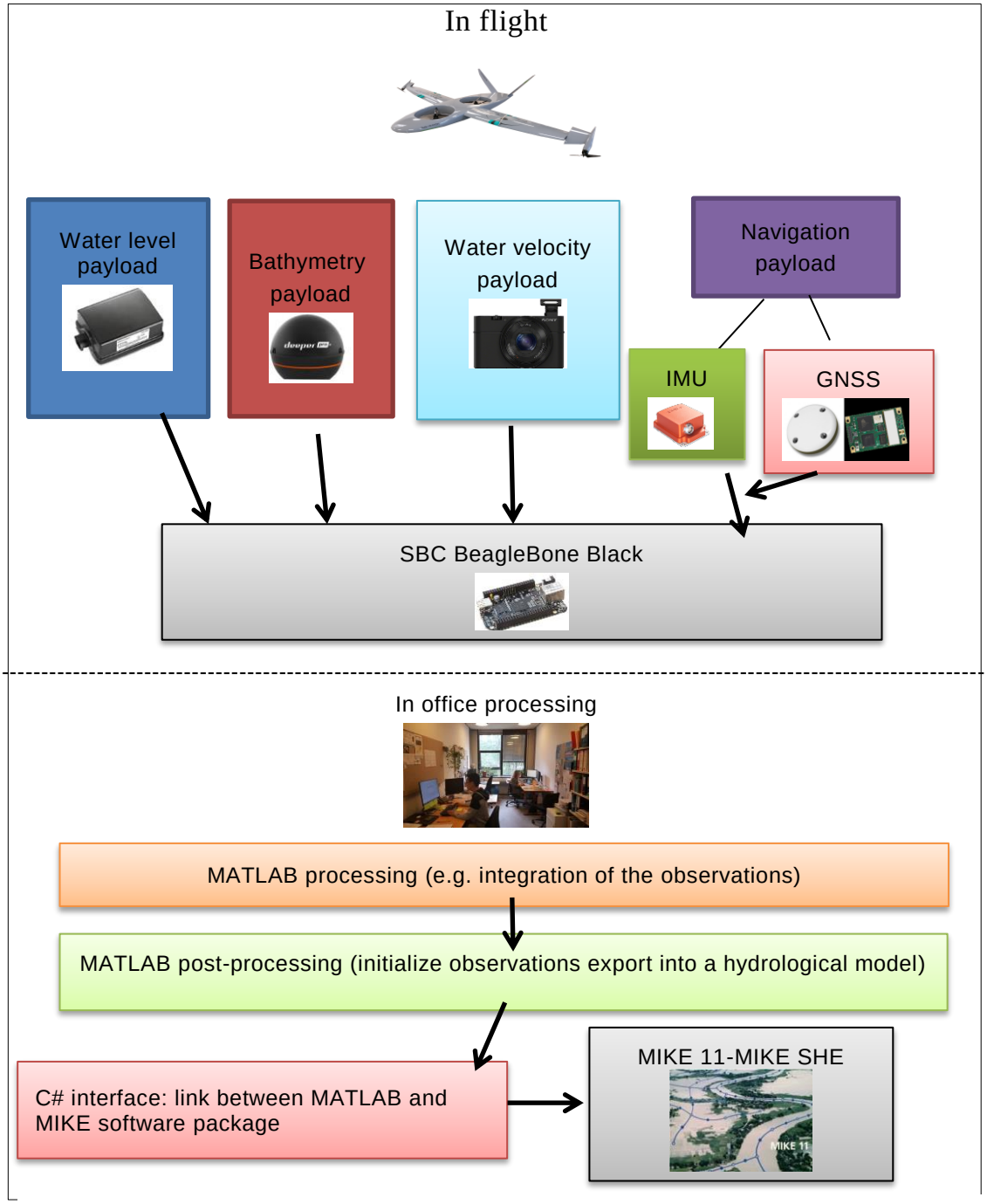

Figure 9. Flowchart of UAV-borne hydraulic observations.

After observations are acquired in flight, processing of the observations is performed through MATLAB software package. As shown in Figure 10 a MATLAB toolbox GUI was developed to process the UAV-borne measurements saved on the SBCs.

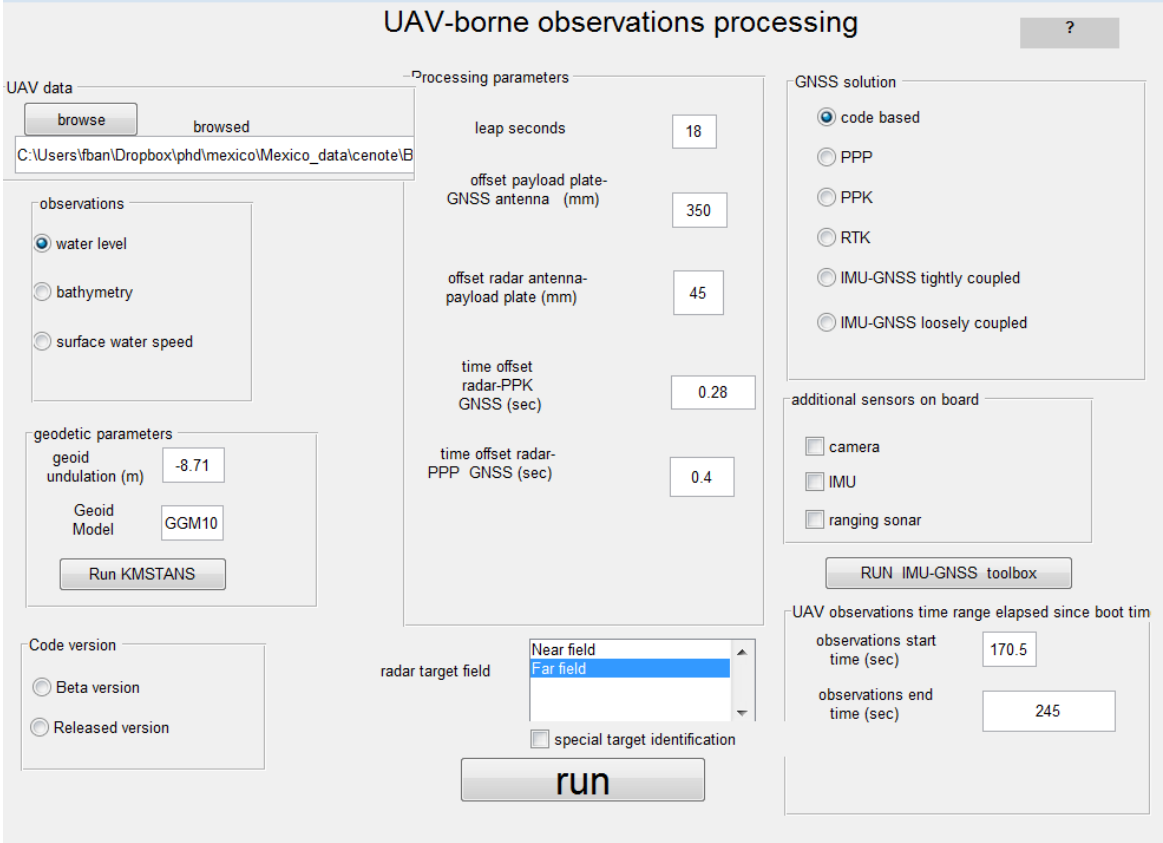

Figure 10. Matlab GUI programmed to process the different UAV-borne hydraulic observations.

The GUI requires the operator to set many parameters: e.g. (i) geoid model and undulation, (ii) vertical offsets between different sensors, (iii) specific time offset constants, (iv) radar settings, (v) algorithms programmed to identify the radar target measuring the water surface, and (vi) GNSS position solution technique. The function of the GUI is to synchronize, geotag the observations and organize them in easily accessible datasets.

A second MATLAB toolbox was developed to initialize the export of the observations into an open-channel model.

This toolbox allows the operator to import: i) The shapefiles containing the river geometry. This shapefile can be obtained either from satellite images (e.g. Google Earth) or from ortho-rectified UAV-borne images (e.g. from AGISOFT PhotoScan software). ii) The river centerline defined in the network .nwk file of MIKE 11 or equivalent software.

In order to export the observations into open-channel models (e.g. Mike 11), the toolbox:

- Mask water level observations using the river geometry shapefiles to remove the land contamination of the radar altimetry observations. Then project the observations onto the river grid 1D computational points (h-points) located at the intersection between each cross section and the river centerline.
- Extract river cross sections from bathymetry observations, maintaining perpendicular alignment to the flow direction.
- Distinguish between the longitudinal and lateral components of the water velocity observations. Convert UAV-borne observations into mean velocity in the vertical water column (applying the correction coefficients available in literature). UAV-borne observations can then be used in 1D models or in fully 2D hydrodynamic models. To be used in 1D model, UAV water velocity observations are projected onto the river centerline.

Figure 11 shows a general river network of an open-channel model.

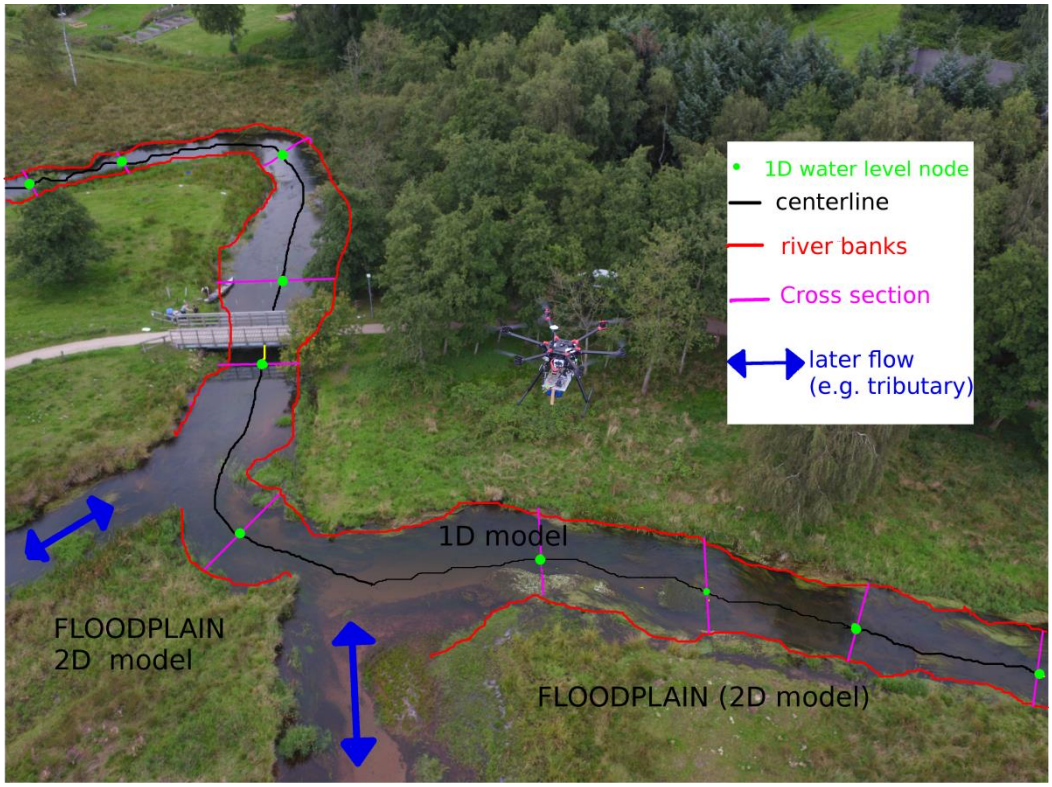

Figure 11. UAV-borne pictures of our DJI Spreading Wings S900 flying over a Danish river (picture credit: Dronesystems.dk). A hydrodynamic 1D model simulates the one-dimensional flow along river centreline, while water level is computed at the computational grid h-points, which are generally located at intersection of each river cross section and centerline. Only 2D models can simulate water levels and velocities in two dimensions i.e. along and perpendicular to the flow. For instance, the flow in floodplains and estuaries is generally simulated with 2D models, while river models are simulated with 1D models.

3.4.1 Calibration of an hydrological model

A river hydrodynamic model was calibrated with UAV-borne water level measurements in Bandini et al. (II) using the DREAM algorithm (Vrugt, 2016; Vrugt et al., 2008). The model parameters were: (i) a spatially uniform Manning coefficient, (ii) datum of the river cross sections, and (iii) river structure (weirs) energy-loss coefficients.

DREAM algorithm was preferred to the SCE (Shuffled Complex Evolution) algorithm (Duan et al., 1993) implemented in the AUTOCAL tool of the MIKE software package. Indeed, DREAM improves the original SCE because it prevents the search in the parameter space from focusing on a small region of attraction and simplifies convergence to a stationary posterior target

distribution. This improved procedure for generation of the candidate points is done through the implementation of the stochastic Metropolis annealing scheme, substituting the SCE replacement procedure that divides the complex into sub-complexes during the generation of the offspring (candidate points).

The UAV-observations and the DREAM algorithm are programmed in MATLAB, but a C#-based GUI was developed to interface the MIKE software package (Mike 11/SHE) with the MATLAB environment. This C#-based software application (Figure 12) also allows for using the river cross section geometries (e.g. cross section datum) as calibration parameters. This option is not available in the original AUTOCAL interface. This GUI requires the operator to: i) define the algorithm settings, ii) set the model calibration parameters, and iii) import the MIKE files (e.g. boundary, hydrodynamic, network and cross section files). Then the GUI allows the user to choose the MIKE SHE file and automatically run the calibration algorithm.

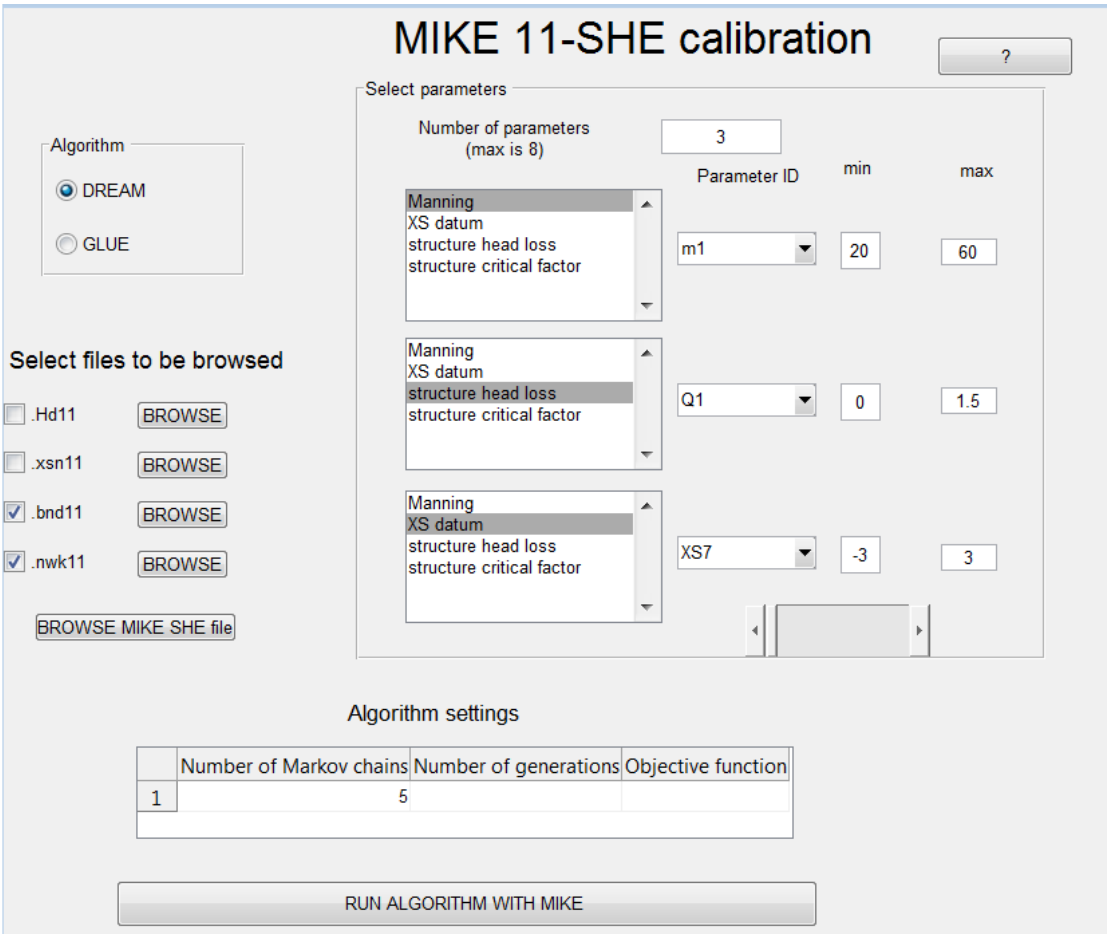

Figure 12. GUI programmed in C# environment to calibrate a Mike11-MIKE SHE model with the Dream or GLUE algorithms. GLUE and DREAM algorithms were provided by the authors (Vrugt, 2016) in MATLAB environment.

4 Results

4.1 Water level observations

In Bandini et al. (I) we tested the potential of different ranging sensors (including our CLDS prototype) for retrieving water level observations by evaluating their accuracy, precision, maximum range capability, and beam divergence. UAV borne tests were mainly performed in a lake located near Holte, Denmark (55.821720° N, 12.509067° E), while static tests were conducted from bridges over free-flowing rivers or other water targets.

The CLDS provided the best results in terms of low beam divergence, which is useful for measuring targets that only expose a small field of view to the ranging sensor. This is the case of narrow rivers or small sinkholes in karst aquifers (e.g. Yucatan peninsula). However, the radar provided the best results in terms of accuracy (0.5% of the range) and maximum range capability (up to 60 m in near field, 200 m in far field). The GNSS system was estimated to have a total vertical uncertainty (TVU) better than 3–5 cm. The overall variance of water level observations is the sum of the radar variance, σ_{rad}^2, and GNSS variance, σ_{GNSS}^2, as shown in (7), assuming that the two error contributions are independent. The overall accuracy was evaluated to be better than 5–7 cm for flights at low altitude (less than 50 m).

$$\sigma_{tot} = \sqrt{\sigma_{rad}{}^2 + \sigma_{GNSS}{}^2} \qquad (7)$$

4.1.1 Study areas for water level observations

Water level observations were retrieved in Mølleåen (Bandini et al., II) to evaluate the potential of our technology for estimating mild water slopes between multiple river structures (weirs) that control the water level of the different Mølleåen stretches.

In Bandini et al. (IV) UAV-borne water level observations were retrieved in the water bodies (cenotes, lagoons, sinkholes) of the Yucatan peninsula. Groundwater and surface water levels on the YP are traditionally collected manually by field operators. However, chronic underfunding, inaccessibility due to dense vegetation, the extensive area, and the poorly developed terrestrial communication network complicate coverage of large areas or establishment of widespread monitoring networks (Bauer-Gottwein et al., 2011; Gondwe et al., 2010). In this kart aquifer, groundwater table is exposed in these surface water bodies, thus UAV-observations are essential to estimate hydraulic gradients between the water bodies and predicting the aquifer streamlines.

In this section, an unpublished study conducted over Vejle Å is reported. The aim of this study was to evaluate the potential of the UAV-borne water surface observations retrieved with our UAV technology (radar and GNSS) compared to water surface observations retrieved with photogrammetry SfM techniques. This study is unpublished because it is a small spatial scale study

(few hundreds of meters). Furthermore, we expect that the accuracy of the observations can be further improved in the next surveys.

This flight was conducted at a height of ca. 30 m above ground level and at an average speed of 2 m/s.

Figure 13 shows that the ortho-photo mosaic obtained from RGB images. Figure 14 shows the DEM obtained from the geotagged RGB images through the SfM software Agisoft PhotoScan. This DEM was obtained without using GCPs. GCPs would potentially improve the accuracy of the photogrammetric DEM to few centimetres, in case they were evenly distributed in the area, including over the water surface. However, GCPs require the operator to access the area and retrieve time-consuming geodetic measurements. Thus, the usage of GCPs was avoided to allow comparison with the UAV-borne altimetry technique, which does not require usage of GCPs.

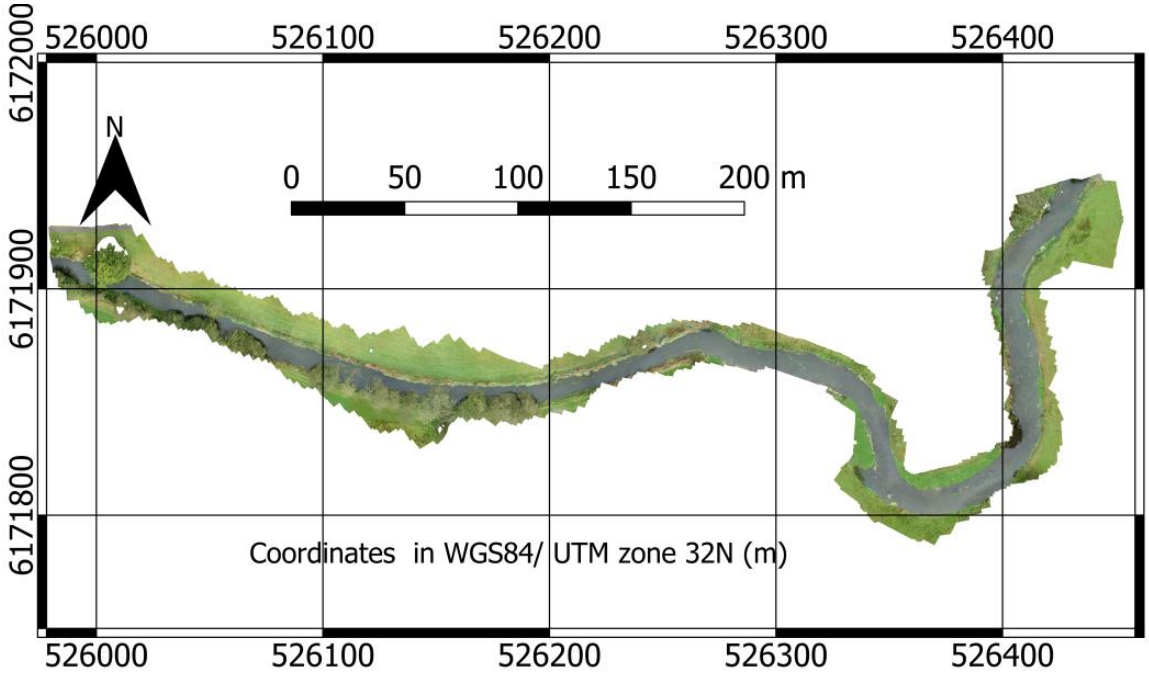

Figure 13. 2D Ortho-mosaic map of UAV-borne RGB images retrieved above a stretch of Vejle Å.

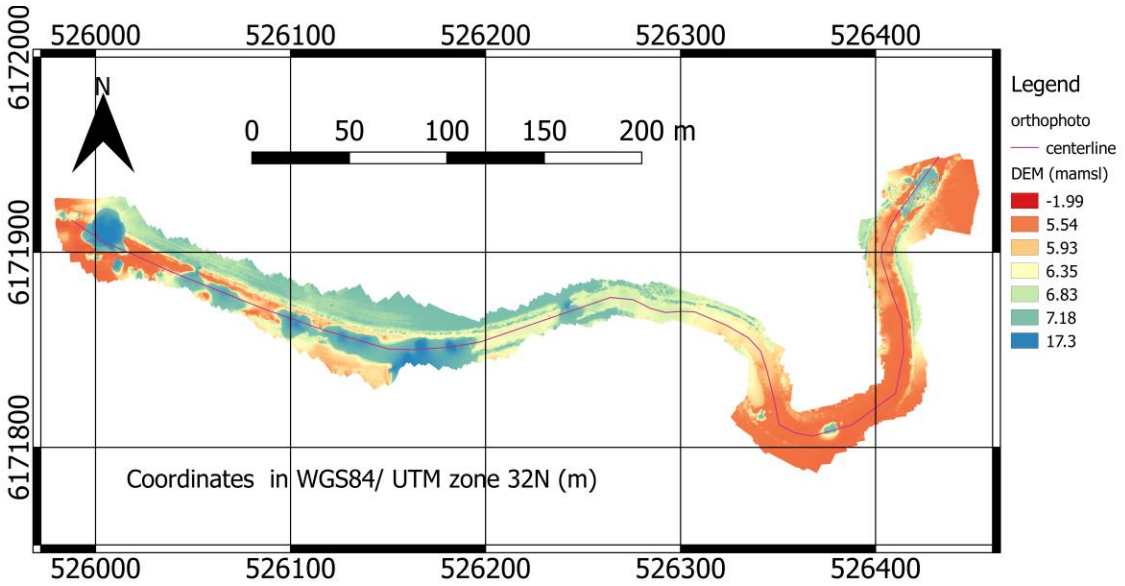

Figure 14. DEM, which shows elevation in meter above mean sea level (mamsl), obtained with photogrammetric SfM technique from UAV-borne RGB images.

Figure 14 shows that the elevation of the water surface is difficult to reproduce with a DEM obtained with the SfM technique. Indeed, photogrammetric DEMs can generally reconstruct the elevation of the land surface with a vertical accuracy of few cm, but water surface is notoriously difficult to reproduce: trees, shadows, aquatic vegetation, and through-water penetration of visible light complicate the reconstruction of the water surface. In Figure 15 we compare (i) the elevation of the water surface along the river centerline obtained with the photogrammetry DEM, (ii) the observations obtained with the water level measuring payload (radar and GNSS system), and (iii) ground truth observations obtained with an RTK GNSS rover station. The accuracy of ground truth observations is ca. ±6 cm.

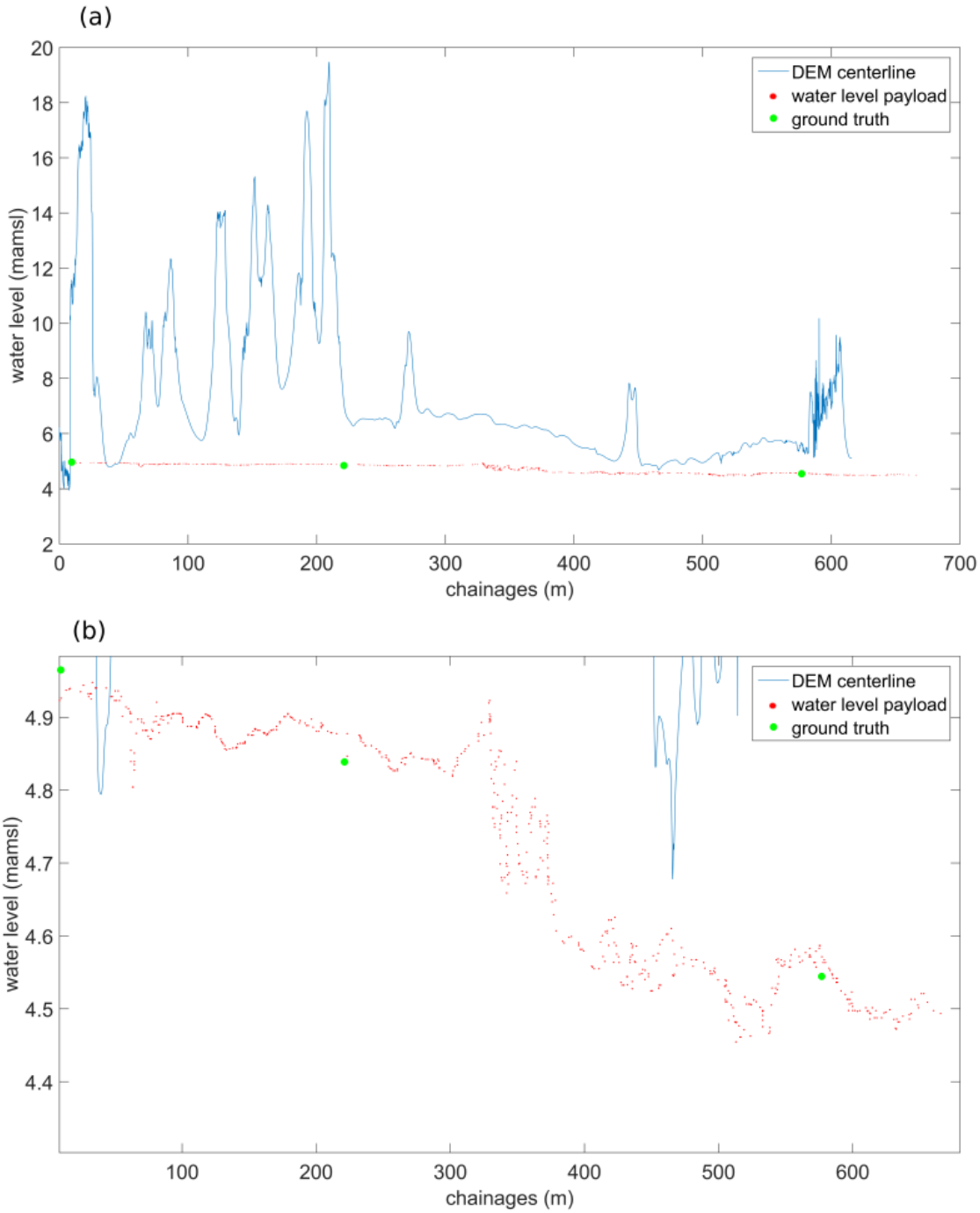

Figure 15 (a) In y axis water level is expressed as meter above mean sea level (mamsl). Red points showed observations retrieved by the UAV water level payload. Blue line is the water level obtained extracting the DEM profile along the river centerline; green dots are ground truth observations. Bottom panel (b) is a detail of (a).

As shown in Figure 16, the DEM reconstruction of the water level slope is disturbed by the vegetation canopy. However, also in areas with a clear field of view to the water surface, the accuracy is ca. 1-1.5 meters. This accuracy

could be potentially improved with the aid of GCPs placed directly on the water surface. However, only the water level measuring payload (radar and GNSS receiver) can reconstruct the water slope, without requiring physical intrusion into the area of interest for placement of GCPs. Indeed, the accuracy of these observations is in the order of 5-7 cm (Bandini et al., I). Nonetheless, our water level measuring payload also records a few climbs and dives. These climbs and dives are due to the inaccuracy of both the radar and the GNSS system. The radar is the main source of uncertainty: it suffers from multipath distortion, interference from riverbanks and canopy, and uncertainty in target identification between the multiple targets in the field of view (Bandini et al., I, II). Similarly, the GNSS receiver has a vertical accuracy of 4-6 cm at 2σ (Bandini et al., I).

4.2 Water depth observations

Water depth (and bathymetry) observations were retrieved in Furesø, in Marrebæk Kanal, Denmark (Bandini et al., III), and in the lagoons and cenotes of the Yucatan peninsula (Bandini et al., IV).

The observations in Bandini et al. (III) were retrieved to evaluate the accuracy of the bathymetric sonar. Observations of the UAV-borne bathymetric sonar were compared with observations retrieved by a bathymetric manned vessel equipped with an accurate bathymetric single-beam sonar. The survey showed good agreement between the two echo-sounders; however, there was a systematic overestimation of water depth for both systems when compared to ground truth observations. The bias factor was shown to be a constant factor for that specific survey and we hypothesize that it was caused by the sound speed dependence on temperature. Our sonar showed an accuracy of 3.8% of the actual depth before this bias factor was corrected, but the accuracy was improved to 2.1% after correction. This confirmed that ground truth observations should be retrieved to correct for site-specific bias factors, e.g. with linear regression. When these corrections are performed, UAV bathymetric surveys are within the accuracy limits established by the International Hydrographic Organization (IHO) for accurate hydrographic surveys. For instance for depths up to ca. 30 m, this 2.1% accuracy complies with the 1st accuracy level. Indeed, for depths of 30 m, our accuracy is of ca. 0.630 m,

while the 1st IHO level standard requires an accuracy better than 0.634 m. Conversely, for depths greater than 30 m, the UAV-borne sonar measurements comply with the 2nd IHO level.

In this section, an unpublished bathymetric survey is reported. A preliminary flight was conducted to evaluate the potential of the UAV-tethered sonar to monitor large (more than 200 m wide) rivers with strong currents and waves. This preliminary flight was conducted above Po river, Italy to evaluate the potential of our technology. Because of logistic constraints, a smaller UAV was flown: a DJI Phantom I. In this case, the on-board GNSS receiver was a single frequency code-based GNSS receiver that resulted in a drone total horizontal uncertainty (THU) of ca. 3-5 m.

In Figure 17 we show the observations of this UAV-borne survey together with the ground truth observations retrieved by Italian "river authorities" with a single-beam on board a manned aquatic vessel in 2005.

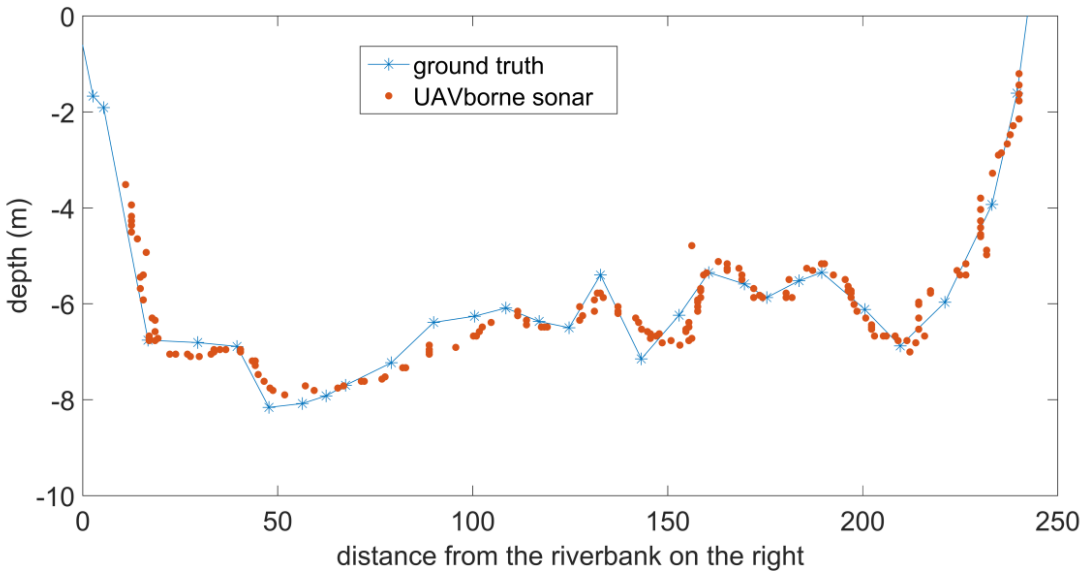

Figure 17. Cross section of Po River, Italy at coordinates 45.073375°, 10.934940° (WGS84 coordinates).

As shown in Figure 17, our sonar is able to retrieve observations also in a large river with strong current. UAV-borne observations show a good agreement with ground truth observations in terms of cross sections shape. However, there are discrepancies in water depth observations. Accuracy estimation of this survey is complicated by the fact that the accuracy of the ground truth observations is unknown and there is a long time gap between the two

datasets. Indeed, ground truth observations were retrieved in 2005 and UAV-borne observations in 2017.

After these accuracy evaluation tests, the sonar sensor was flown in Yucatan peninsula to measure the water depth (and bathymetry) of the Mexican water bodies (Bandini et al. IV).

4.3 Water speed observations

Researchers have already applied LSPIV method to UAV-borne imagery to estimate surface velocity. Detert and Weitbrecht (2015) found a strong agreement between UAV-borne LSPIV water surface velocity profiles extracted along river cross sections and ADCP measurements. Tauro et al. (2016b) compare UAV-borne LSPIV with surface speed measurements obtained with a current meter. Maximum surface velocity measured with UAV-borne LSPIV was 2.29 m/s ($\sigma\approx0.09$ m/s) when artificial tracers were used and 2.15 m/s ($\sigma\approx0.27$ m/s) with natural tracers (leaves). The current meter, which was positioned in the centre of the river ca. 3 cm underneath the water surface (i.e. where speed is less influenced by the wind), recorded a velocity of 2.54 m/s ($\sigma\approx0.09$ m/s).

Bolognesi et al. (2016) compared LSPIV measurements with total station and dual camera close range photogrammetry observations of an artificial tracer (floating object positioned in the centre of the river where velocity is higher). The total station and the close range photogrammetry were in strong agreement, with a difference in velocity estimation of less than 9%. UAV-observations showed good agreement with the total station, with an error generally less than 10% and with a remarkable percentage error in one location ($\approx$ 26.5%) probably due to the low water speed in that location ($\approx$0.009 m/s). Low speed is a critical factor in LSPIV. LSPIV generally requires that water appears to be flowing to a naked eye. However, in low water speed conditions, tracers are strongly affected by the wind and the observed velocity field might not be representative of the water surface. Bolognesi et al. (2016) also compare UAV-borne LSPIV estimates obtained with and without GCPs. When the UAV altitude is known, the percentage difference is ca. 6-7% between LSPIV with and without GCPs.

A preliminary survey was conducted to retrieve surface water speed with UAV-borne LSPIV. These surveys were important to identify the best camera settings, drone flight height, image stabilization algorithm, and seeding technique.

Videos were captured in Mølleåen river, Lille Skensved, and in Store Vejle Å. Mølleåen river did not show as sufficient water speed for application of LSPIV during the survey season. Thus, only in Lille Skensved and Store Vejle Å the magnitude of water flow was sufficient for application of LSPIV.

A 3-axis gimbal can decrease low-frequency angular motion of the camera, but cannot eliminate high-frequency vibrations, thus it was not used. Proper damping of the drone payload was essential to decrease high-frequency motion and avoid large error in LSPIV. Furthermore, drone vibrations and drifts were removed by stabilizing videos in post-processing mode. Stable features (e.g. small rocks or artificial panels) along the riverbank were used as reference points.

In Figure 18 we show a video sequence retrieved in Lille Skensved (55°30'50.8"N 12°09'06.1"E). The video was stabilized using the two GCPs (metal panels) shown in the frames. The flight was conducted from an altitude above the water surface of 15.25 m (with a σ=0.1 m). Water was "seeded" with woodchips.

Figure 18. UAV-borne video capture (50 frames per seconds). Each panel shows water surface every 0.10 s. Red rectangles highlight the GCPs.

The horizontal and vertical coordinates of these GCPs were measured with an RTK rover GNSS station. The accurate coordinates of the GCPs allowed us

to convert the displacement vectors from pixel units into real-world distance units. The 2D velocity field is shown in Figure 19.

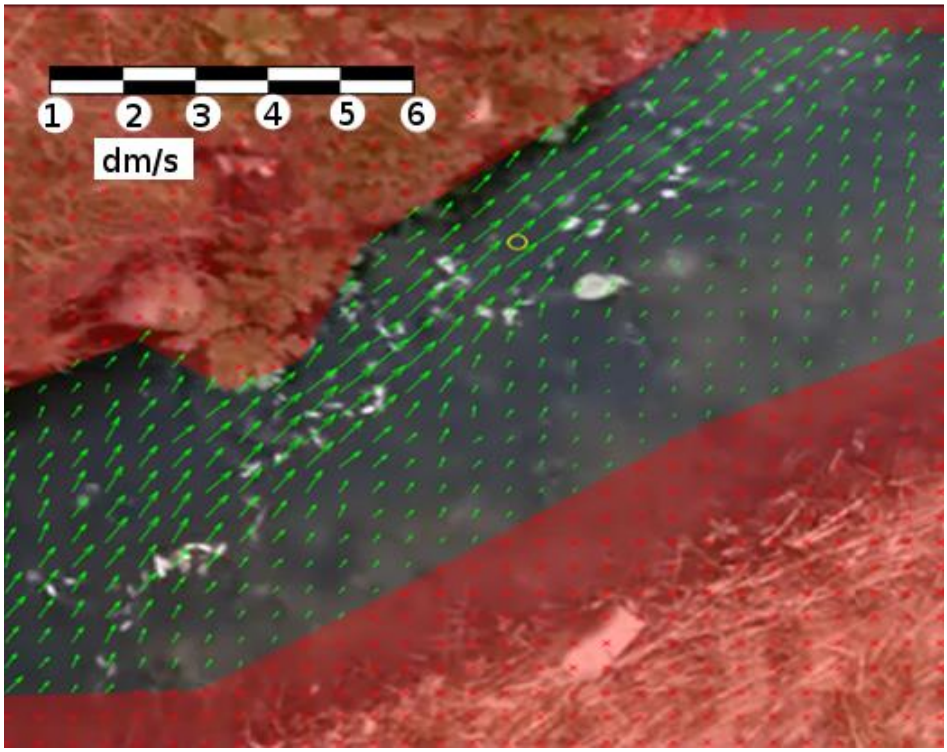

Figure 19. 2D velocity field computed with LSPIV technique from the video frames of Figure 18.

Figure 20 shows the locations at which video sessions were captured in Store Vejle Å. Two video sections were captured from the drone (I and III) from an altitude above the water surface of 10.35 m (with a σ=0.05 m), and one video was captured from a stationary position located on a bridge (II) from a height above the water surface of 2.60 m.

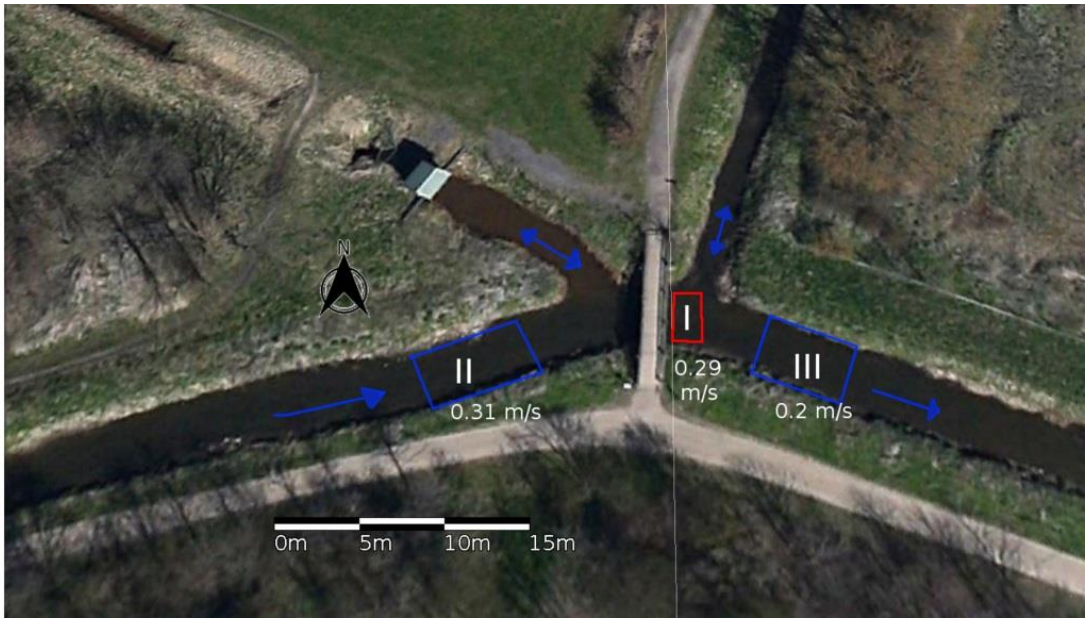

Figure 20. Modified from Holm and Goosmann (2016). Location (I, II, III) at which videos were taken. Image location is 55.626° N 12.362° E (WGS84 coordinates).

In this case study, we avoided the usage of GCPs. Indeed, the radar recorded the altitude above the water surface during each video section. Equations of Table 2 were used to convert from image units into metric units.

Table 3 shows the mean velocity and the error statistics computed at the three locations.

Table 3. Mean longitudinal velocity (μ) and statistics retrieved with LSPIV at the three different locations. CV stands for coefficient of variation (ratio between the standard deviation in velocity and μ) and σ_{dir} is the standard variation in the direction angle of the computed vectors. CV and σ_{dir} are shown as mean value of the velocity field vectors retrieved at each specific location.

Video number	μ [m/s]	mean CV [-]	mean σ_{dir} [rad]
I (static)	0.29	0.06	0.06
II (UAV-borne)	0.31	0.19	0.19
III (UAV-borne)	0.20	0.20	0.29

Table 3 shows that the river significantly decreases its velocity downstream. From the location under the bridge (I) to the location after the bridge (III) average water speed decreases by ca. 0.09 m/s. This is probably due to the tributary river between the two locations. Furthermore, it appears that the CV and the σ_{dir} with UAV-borne videos are significantly higher than with the

static video from the bridge. This is certainly due to the UAV vibrations and drifts, which result in larger error statistics.

Figure 21 depicts the 2D velocity field for the video retrieved at section III.

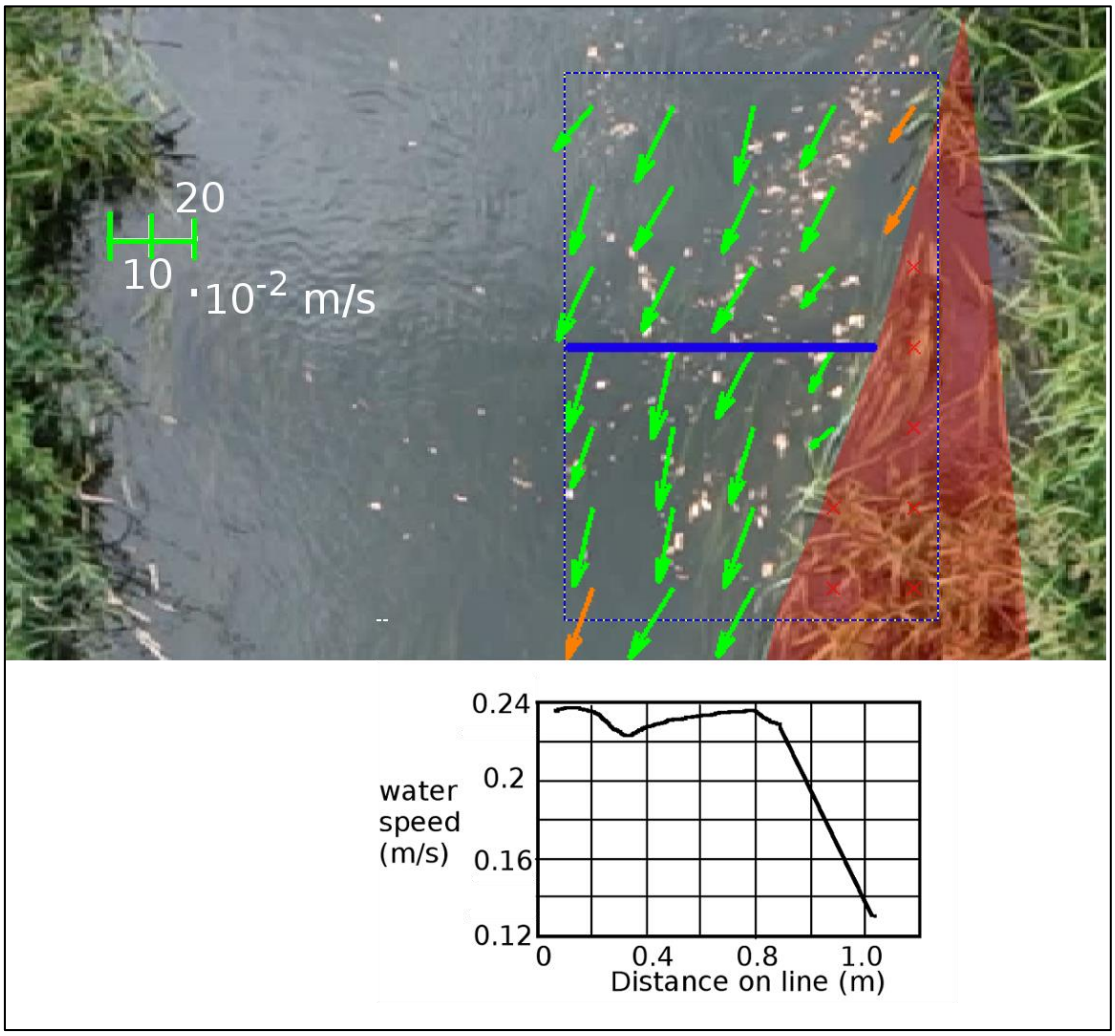

Figure 21. Modified from Holm and Goosmann (2016). Top panel shows 2D velocity field retrieved with UAV-borne LSPIV. Bottom graph shows the profile of water speed extracted along the blue line.

Figure 21 shows that the LSPIV algorithm estimates the water velocity vectors only in the region in which the tracers (woodchips) are identifiable. Indeed, in this case study, water velocity was underestimated by a factor of 10, and the overall standard deviation, both for the velocity magnitude and the direction of the water velocity vectors, is increased by a factor of 10 in regions without any woodchips (Holm and Goosmann, 2016).

However, Lüthi et al. (2014) have recently developed a new image cross-correlation analysis algorithm for LSPIV. The authors claim that it does not require the usage of any artificial seeding, but it can compute the velocity field by examining debris, bubbles, and turbulence structures. The algorithm provides accurate velocity observations for a wide range of water conditions, provided that water appears to be flowing to the naked eye. However, this algorithm was not tested on UAV-borne imagery and typically requires a side-looking camera (Philippe et al., 2017).

4.4 Calibration and validation of hydrological models with UAV-borne observations

UAV observations of river hydraulics are a fairly new field. For this reason, few scientific works evaluate the potential of these new datasets for informing hydrodynamic open-channel models. While bathymetry observations can generally be used to directly inform hydrodynamic models, orthometric water level (or water slope) and surface velocity are outputs of river models. However, these observations are essential to (i) improve knowledge of the distribution of model parameters through model calibration or (ii) adjust model state variables through data assimilation.

A synthetic study was conducted Bandini et al. (II) to evaluate the potential of UAV-borne water level observations for calibrating an integrated hydrological model (Mølleåen river and its catchment, Denmark) and improve estimates of GW-SW interaction. Our study reported an improvement in the sharpness and reliability of the model estimates after calibration against water level observations. In particular, the RMSE decreases by ca. 75%, the direction of the exchange flux is better simulated, and sharpness is improved by 50% compared to a model calibrated against discharge only. Indeed calibration against water level observations with high spatial resolution improved knowledge about the distribution of the model parameters (specifically Manning coefficient, river structure coefficients, geodetic datum of river cross sections).

In Bandini et al. (IV) water level and bathymetry observations were obtained in the water bodies of the Yucatan peninsula. This research paper demon-

strated that cenotes and lagoons of the Yucatan peninsula can be surveyed with UAVs equipped with our payloads. UAVs can monitor water level and bathymetry of these surface water bodies at a regional scale, without requiring the operator to access the area and establish levelling networks or use water level dip meters. Water level observations in this karstic aquifer improved estimations of hydraulic gradients and groundwater flow directions in the surveyed area. Correspondingly, measurements of bathymetry and water depth were capable of improving current knowledge of the complicated submerged cave systems of the karst aquifer. For instance, anomalies in water depths allowed identification of fractures in the limestone rock that resulted in deeper cenotes or caves inside shallow lagoons (Bandini et al. IV).

5 Discussion

Figure 22 shows the advantages of UAVs compared to satellite, in-situ, and airborne measurements.

Satellites observations ensure (i) large -scale coverage but, but are constrained by (ii) low accuracy and (iii) low resolution, with (iv) a temporal coverage that depends on the repeat cycle and (v) a spatial coverage that depends on the orbit. Furthermore, space-borne sensors are currently unable to measure bathymetry or water speed.

In-situ measurements are local point measurements, thus they do not capture spatial patterns.

Airborne measurements offer a high spatial resolution at a moderate spatial scale, but are very expensive.

Rotary wing UAVs can monitor targets with (a) optimal accuracy and (b) resolution, (c) good manoeuvrability and (d) high flexibility, but cannot fly long ranges.

Finally, hybrid platforms (e.g. SmartUAV) combine the advantages of fixed wing with advantages of rotary wing UAVs. Indeed hybrid platforms can fly long distance with low energy consumption and BVLOS capability (as fixed wing), and with VTOL capability (as rotary wing).

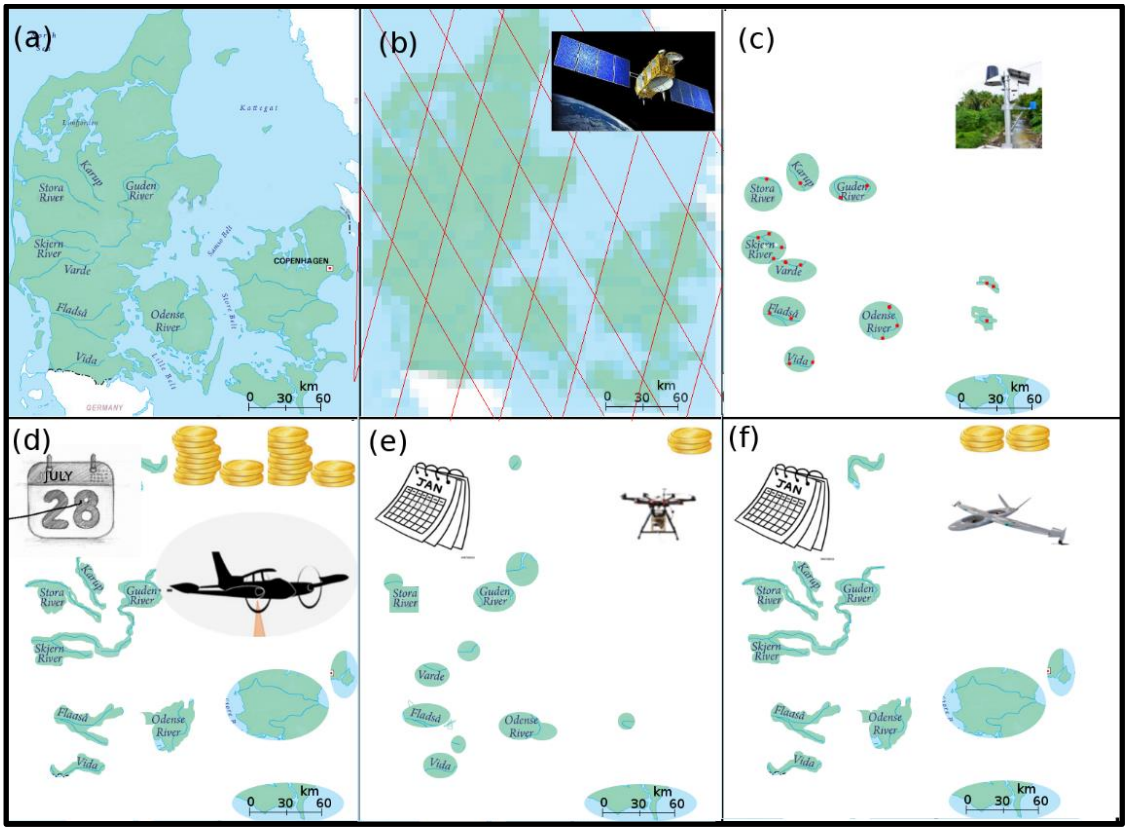

Figure 22. Comparison between different techniques to measure water level. (a) Map of Denmark with highlighted the major Danish rivers. (b) Satellite measurements ensure large spatial scale, with a spatial coverage depending on the orbit patterns (red strips). Low spatial resolution and accuracy are the main constraints. (c) In-situ measurements can capture only local 1D observations (red points). (d) Airborne survey can retrieve accurate observations but are expensive and therefore cannot be conducted frequently. (e) Rotary wings UAVs are low-cost and flexible platforms that can retrieve accurate observations with high spatial resolution but at low spatial scale due to the flight time and range constraints. Mission repeatability is ensured (i.e. high temporal resolution is achievable). (f) Hybrid fixed and rotary-wings UAVs (e.g. SmartUAV) ensure accurate observations with large spatial coverage at a limited cost. Mission repeatability is also ensured.

Map of Denmark: modified from https://www.mapsofworld.com. Satellite image source: Artist's view of the Jason-2 spacecraft (image credit: CNES). Airplane image credit: http://felix.rohrba.ch

5.1 UAV-borne water level

Our research proved that water level can be retrieved from UAV with high spatial resolution and accuracy. Due to size and weight limitations of commercial LIDAR systems, radar sensors can be considered as the best solution for monitoring water level with high accuracy from UAVs.

Table 4 compare our UAV-borne technology with other remote sensing techniques.

Table 4. Accuracy and ground footprint of different techniques for observing water level. Source: Bandini et al., I.

Location	Technique	Ground footprint	Accuracy	Reference
Airborne	LIDARs	20 cm-1 m	4-22 cm	(Hopkinson et al., 2011)
Spaceborne	laser altimetry (ICESat)	50–90 m	10-15 cm	(Phan et al., 2012)
Spaceborne	radar altimetry (e.g. ERS2, Envisat, Topex/Poseidon)	400 m-2 km	30-60 cm	(Frappart et al., 2006)
Ground-based	radar/sonar/pressure transducers	mm-cm	1 mm-10 cm	Widely known metrology
UAV-borne	radar altimetry	dm-m	5-7 cm	Bandini et al., I, II, IV

Table 4 shows that UAVs have an accuracy and spatial resolution better than other space-borne and airborne technologies. Thus, UAVs can be the optimal solution for flood mapping because they allow for high spatial resolution but also optimal timing of the observations.

5.2 UAV-borne water depth

Our tethered sonar controlled by a UAV is a promising technique. It showed an accuracy better than other remote sensing techniques (LIDARs, though-water photogrammetry, depth-spectral signature), with the additional advantage that it is suitable for all water conditions and a large range of depths.

Table 5 summarizes the potential of our UAV-borne system compared to other remote sensing techniques.

Table 5. Comparison of different remote sensing technique to retrieve hydraulic observations. Modified from Bandini et al. (III).

Technique	Max. water depth (m)	Typical error (m)	Applicability	References
Spectral signature	1-1.50	0.10-0.20	Clear water	Satellite: (Fonstad and Marcus, 2005; Legleiter and Overstreet, 2012) Aircraft: (Carbonneau et al., 2006; Legleiter and Roberts, 2005; Winterbottom and Gilvear, 1997) UAV: (Flener et al., 2013; Lejot et al., 2007)
Through-water photogrammetry	1-1.50	0.08-0.2	Gravel-bed water bodies with extremely clear water	Aircraft: (Feurer et al., 2008; Lane et al., 2010; Westaway et al., 2001) UAV: (Bagheri et al., 2015; Dietrich, 2016; Tamminga et al., 2014; Woodget et al., 2015)
LIDAR	1-1.5	≈13	Gravel-based water bodies with very clear water: 1-1.5 Secchi Depth	UAV: (Mandlburger et al., 2016)
	6	0.05-0.3	Clear water	Aircraft: (Bailly et al., 2012, 2010; Charlton et al., 2003; Hilldale and Raff, 2008; Kinzel et al., 2007)
Sonar tethered to UAV	0.5-80	≈3.8%[d] ≈2.1%[e] of actual depth	All water conditions	(Bandini et al., III)

[d]before bias factor correction

[e]after bias factor correction

Our UAV technology ensures the possibility to retrieve water depths at a moderate spatial scale (e.g. 0.001-3 km) in areas that are hardly accessible to humans, and in streams that are not navigable because of strong currents or obstacles (e.g. river structures). This is the main advantage compared to aquatic manned or unmanned vessels (e.g. Brown et al. 2010; Ferreira et al. 2009; Giordano et al. 2015) equipped with echo-sounders.

5.3 Surface water speed

Our preliminary study on UAV-borne LSPIV showed results in agreement with other similar studies (Detert and Weitbrecht, 2015; Tauro et al., 2016b, 2015a, 2015b). Our approach did not require the usage of GCPs, the coordinates of which should be measured with geodetic techniques, for image calibration and geo-rectification. To overcome the need for GCPs, the range to the water surface, which is measured by the on-board radar, was used for conversion from image units (pixels) into metric units.

Our preliminary studies show that UAV-borne LSPIV requires: i) seeding of the water surface in case no natural tracers are available and ii) stabilization of image vibrations.

Indeed, the low velocity and the absence of natural tracers in Danish streams generally require the seeding with artificial tracers (e.g. woodchips) for application of traditional LSPIV techniques. Researchers (Jodeau et al., 2008; Meselhe et al., 2004) suggested that 10-30% of the water surface should be covered by tracers to avoid major errors in the estimation of surface velocities for application of LSPIV in free-flowing rivers. Artificial seeding of the water surface is a strong constraint; indeed, it requires the operator to access the area or the UAV to discharge woodchips over the water surface.

Vibrations and small drifts of the UAV are the most problematic effect that requires correction. The captured UAV-borne videos were stabilized using static reference points (e.g. small rocks), which can be generally found on the riverbanks. However, image stabilization techniques are not always capable of removing drone vibrations.

6 Conclusions

UAVs are interesting platforms for monitoring hydraulic variables, because they ensure (i) high spatial resolution (ii) high accuracy (iii) high flexibility, and (iv) low cost of operations. These are the main advantages compared to

satellite or airborne remote sensing methods. Furthermore, UAVs can acquire real time observations also during extreme events (only when rain and wind do not exceed maximum safe limits for flights) and ensure a good tracking of surface water bodies. Our research shows that UAVs can monitor hydraulic variables of inland water bodies, in particular:

- UAVs equipped with a W-band radar and GNSS system can measure water level at high spatial resolution with an accuracy better than 5-7 cm.
- Water depths can be monitoring by a tethered sonar system, which is controlled by the UAV, with an accuracy of ca. 2.1 % of actual depth for depths potentially up to 80 m. For depths up to 30 m, this relative error is in agreement with the 1st level accuracy of the IHO standards.
- 2D surface speed field can be measured with the LSPIV technique applied to UAV-borne video frames. However, seeding of the water surface by artificial tracers (e.g. woodchips) can be avoided only when a natural occurrence of tracers (e.g. bubbles, foam, or differences in water colour generated by water suspended solids) exists.

UAV observations can be used to inform hydraulic open-channel models. Bathymetry can be directly used to inform the hydraulic model, while UAV-borne water level and speed can be used to calibrate and validate the model outputs.

Two hydrological studies were conducted to evaluate the potential of:

- UAV-borne water level observations in calibrating a model of a Danish river. Calibration against these observations improved sharpness and reliability of the groundwater (GW)-surface water (SW) model estimates.
- UAV-borne water level and depth observations in monitoring the karst aquifer of the Yucatan peninsula. Observations of water level were required to estimate hydraulic gradients and groundwater flow directions, while bathymetry and water depth observations improved current knowledge on how the surface water bodies connect through the complicated submerged cave systems and the diffuse flow in the rock matrix.

Water depth and surface velocity can also serve as surrogate for discharge estimation. However, in order to estimate discharge, hydrodynamic equations are needed to convert surface velocity into mean velocity.

Thus, this thesis shows that UAV-base remote sensing is an approach that combines the advantages of in-situ methods, such as accuracy and high temporal resolution, with the advantages of remote sensing techniques, such as spatial coverage. Hydraulic observations with (i) high accuracy (ii) high spatial resolution (iii) medium to large spatial scale coverage cannot be retrieved with traditional techniques and necessitate the employment of UAVs. In the future, advanced miniaturized sensors will further improve the accuracy of the UAV-borne observations, whereas UAV automation will ensure duration, repeatability, and coverage of flight missions.

7 Future challenges

The ±5-7 cm accuracy of our UAV-borne water level technology is better than other remote sensing techniques. However, it may still be insufficient to monitor water slope in rivers flowing through low-lying terrain (Bandini et al., I, II). Nonetheless, advanced miniaturized components are expected to improve the accuracy of radar systems and GNSS receivers/antennas; thus, an accuracy below 5-7 cm can potentially be reached in the near future. For instance, compact lightweight radar exploiting the microwave regions that are normally used in satellite water altimetry (e.g. Ku, C and Ka bands) should be soon available on the market. These radar systems might be able to retrieve water surface with 1-2 cm accuracy for flight heights up to 100 m. In this regard, the accuracy of the GNSS system appears to be the main limitation to the overall accuracy in the long term.

UAV-depth observations are very promising for the achieved accuracy and for their applicability in a wide range of water conditions. However, the usage of a tethered sonar is risky because it requires a flight height that is only few meters above the water surface. Nevertheless, sonar technology is so far the most accurate and versatile technology in measuring bathymetry. In the near future, new compact bathymetric LIDARs might enter the UAV market, but it is unlikely that they will be capable of measuring bathymetry when the actual depth is several times the Secchi depth, i.e. in the majority of rivers.

Researchers have already conducted studies on how to retrieve surface water speed with UAV-borne LSPIV. However, payload damping systems and video stabilization techniques should be improved to remove drone vibrations and drifts. Furthermore, the usage of artificial tracers is not practical because it requires the operator to access the area. Thus UAV-LSPIV should apply algorithms (e.g. Fujita and Kunita, 2011; Philippe et al., 2017) that do not require the usage of artificial tracers, but identify the water movement by taking advantage of turbulence ripples, differences in colour due to suspended sediments and natural debris.

7.1 Developments in UAV platforms

The full potential of UAVs will be exploited when autonomous flight systems and computer vision systems allow UAVs to retrieve observations without requiring the operator to access the area. Indeed, BVLOS flights are very promising, especially in regions that are difficult to access (e.g. Mexican cenotes). In the near future, we expect UAVs to be capable of flying and being recharged automatically when hyper-spatial observations of water depth, level, and bathymetry need to be retrieved. Thus, UAVs offer high spatial resolution and accuracy, in addition to the possibility to cover large areas and repeat the flight missions frequently.

8 References

Alsdorf, D.E., Rodriguez, E., Lettenmaier, D.P., 2007. Measuring surface water from space. Rev. Geophys. 45, 1–24. doi:10.1029/2006RG000197.1

Baghdadi, N., Lemarquand, N., Abdallah, H., Bailly, J.S., 2011. The Relevance of GLAS/ICESat Elevation Data for the Monitoring of River Networks. Remote Sens. 3, 708–720. doi:10.3390/rs3040708

Bagheri, O., Ghodsian, M., Saadatseresht, M., 2015. Reach scale application of UAV+SfM method in shallow rivers hyperspatial bathymetry, in: International Archives of the Photogrammetry, Remote Sensing and Spatial Information Sciences - ISPRS Archives. pp. 77–81. doi:10.5194/isprsarchives-XL-1-W5-77-2015

Bailly, J.-S., Kinzel, P.J., Allouis, T., Feurer, D., Le Coarer, Y., 2012. Airborne LiDAR Methods Applied to Riverine Environments, in: Fluvial Remote Sensing for Science and Management. pp. 141–161. doi:10.1002/9781119940791.ch7

Bailly, J.S., le Coarer, Y., Languille, P., Stigermark, C.J., Allouis, T., 2010. Geostatistical estimations of bathymetric LiDAR errors on rivers. Earth Surf. Process. Landforms 35, 1199–1210. doi:10.1002/esp.1991

Banic, J., 1998. Airborne laser bathymetry: A tool for the next millennium. EEZ Technol. 75–80.

Bauer-Gottwein, P., Gondwe, B.R.N., Charvet, G., Marin, L.E., Rebolledo-Vieyra, M., Merediz-Alonso, G., 2011. Review: The Yucatan Peninsula karst aquifer, Mexico. Hydrogeol. J. 19, 507–524. doi:10.1007/s10040-010-0699-5

Berni, J.A.J., Member, S., Zarco-tejada, P.J., Suárez, L., Fereres, E., 2009. Thermal and Narrowband Multispectral Remote Sensing for Vegetation Monitoring From an Unmanned Aerial Vehicle. Geosci. Remote Sens. 47(3), 722–738. doi:10.1109/TGRS.2008.2010457

Berry, P.A.M., Garlick, J.D., Freeman, J.A., Mathers, E.L., 2005. Global inland water monitoring from multi-mission altimetry. Geophys. Res. Lett. 32, 1–4. doi:10.1029/2005GL022814

Biancamaria, S., Frappart, F., Leleu, A.S., Marieu, V., Blumstein, D., Desjonqu??res, J.D., Boy, F., Sottolichio, A., Valle-Levinson, A., 2017. Satellite radar altimetry water elevations performance over a 200??m wide river: Evaluation over the Garonne River. Adv. Sp. Res. 59, 128–146. doi:10.1016/j.asr.2016.10.008

Birkett, C.M., 1998. Contribution of the TOPEX NASA Radar Altimeter to the global monitoring of large rivers and wetlands. Water Resour. Res. 34, 1223. doi:10.1029/98WR00124

Birkett, C.M., Mertes, L. a K., Dunne, T., Costa, M.H., Jasinski, M.J., 2002. Surface water dynamics in the Amazon Basin: Application of satellite radar altimetry. J. Geophys. Res. Atmos. 107, LBA-26. doi:10.1029/2001JD000609

Birkinshaw, S.J., O'Donnell, G.M., Moore, P., Kilsby, C.G., Fowler, H.J., Berry, P.A.M., 2010. Using satellite altimetry data to augment flow estimation techniques on the Mekong River. Hydrol. Process. 24, 3811–3825. doi:10.1002/hyp.7811

Bjerklie, D.M., Moller, D., Smith, L.C., Dingman, S.L., 2005. Estimating discharge in rivers using remotely sensed hydraulic information. J. Hydrol. 309, 191–209. doi:10.1016/j.jhydrol.2004.11.022

Bolognesi, M., Farina, G., Alvisi, S., Franchini, M., Pellegrinelli, A., Russo, P., 2016. Measurement of surface velocity in open channels using a lightweight remotely piloted aircraft system Measurement of surface velocity in open channels using a lightweight remotely piloted aircraft system. Geomatics, Nat. Hazards risk 5705. doi:10.1080/19475705.2016.1184717

Brooks, R., 1982. Lake elevation from satellite radar altimetry from a validation area in Canada. Salibury, Maryland, USA.

Brown, H.C., Jenkins, L.K., Meadows, G.A., Shuchman, R.A., 2010. BathyBoat: An autonomous surface vessel for stand-alone survey and underwater vehicle network supervision. Mar. Technol. Soc. J. 44, 20–29.

Calmant, S., Seyler, F., 2006. Continental surface waters from satellite altimetry. Comptes Rendus - Geosci. 338, 1113–1122. doi:10.1016/j.crte.2006.05.012

Calmant, S., Seyler, F., Cretaux, J.F., 2008. Monitoring continental surface waters by satellite altimetry. Surv. Geophys. 29, 247–269. doi:10.1007/s10712-008-9051-1

Carbonneau, P.E., Lane, S.N., Bergeron, N., 2006. Feature based image processing methods applied to bathymetric measurements from airborne remote sensing in fluvial environments. Earth Surf. Process. Landforms 31, 1413–1423. doi:10.1002/esp.1341

Charlton, M.E., Large, A.R.G., Fuller, I.C., 2003. Application of airborne lidar in river environments: The River Coquet, Northumberland, UK. Earth Surf. Process. Landforms 28, 299–306. doi:10.1002/esp.482

Cheviron, B., Moussa, R., 2016. Determinants of modelling choices for 1-D free-surface flow and morphodynamics in hydrology and hydraulics: A review. Hydrol. Earth Syst. Sci. doi:10.5194/hess-20-3799-2016

Chiu, C.-L., 1988. Entropy and 2-D Velocity Distribution in Open Channels. J. Hydraul. Eng. 114, 738–756. doi:10.1061/(ASCE)0733-9429(1988)114:7(738)

Chow, V.T., 1959. Open Channel Hydraulics. McGraw-Hill B. Co. doi:ISBN 07-010776-9

Colomina, I., Molina, P., 2014. Unmanned aerial systems for photogrammetry and remote sensing: A review. ISPRS J. Photogramm. Remote Sens. 92, 79–97. doi:10.1016/j.isprsjprs.2014.02.013

Creutin, J.D., Muste, M., Bradley, A.A., Kim, S.C., Kruger, A., 2003. River gauging using PIV techniques: A proof of concept experiment on the Iowa River. J. Hydrol. 277, 182–194. doi:10.1016/S0022-1694(03)00081-7

Detert, M., Weitbrecht, V., 2015. A low-cost airborne velocimetry system: proof of concept. J. Hydraul. Res. 53, 532–539. doi:10.1080/00221686.2015.1054322

Dietrich, J.T., 2016. Bathymetric Structure from Motion: Extracting shallow stream bathymetry from multi-view stereo photogrammetry. Earth Surf. Process. LandformsEarth Surf. Process. Landforms. doi:10.1002/esp.4060

Duan, Q.Y., Gupta, V.K., Sorooshian, S., 1993. Shuffled complex evolution approach for effective and efficient global minimization. J. Optim. Theory Appl. 76, 501–521. doi:10.1007/BF00939380

Durand, M., Fu, L.L., Lettenmaier, D.P., Alsdorf, D.E., Rodriguez, E., Esteban-Fernandez, D., 2010. The surface water and ocean topography mission: Observing terrestrial surface water and oceanic submesoscale eddies, in: Proceedings of the IEEE. pp. 766–779. doi:10.1109/JPROC.2010.2043031

Durand, M., Andreadis, K.M., Alsdorf, D.E., Lettenmaier, D.P., Moller, D., Wilson, M., 2008. Estimation of bathymetric depth and slope from data assimilation of swath altimetry into a hydrodynamic model. Geophys. Res. Lett. 35. doi:10.1029/2008GL034150

Ferreira, H., Almeida, C., Martins, A., Almeida, J., Dias, N., Dias, A., Silva, E., 2009. Autonomous bathymetry for risk assessment with ROAZ robotic surface vehicle, in: OCEANS '09 IEEE Bremen: Balancing Technology with Future Needs. doi:10.1109/OCEANSE.2009.5278235

Feurer, D., Bailly, J.-S., Puech, C., Le Coarer, Y., Viau, a. a., 2008. Very-high-resolution mapping of river-immersed topography by remote sensing. Prog. Phys. Geogr. 32, 403–419. doi:10.1177/0309133308096030

Flener, C., Vaaja, M., Jaakkola, A., Krooks, A., Kaartinen, H., Kukko, A., Kasvi, E., Hyyppä, H., Hyyppä, J., Alho, P., 2013. Seamless mapping of river channels at high resolution using mobile liDAR and UAV-photography. Remote Sens. 5, 6382–6407. doi:10.3390/rs5126382

Flynn, K.F., Chapra, S.C., 2014. Remote sensing of submerged aquatic vegetation in a shallow non-turbid river using an unmanned aerial vehicle. Remote Sens. 6, 12815–12836. doi:10.3390/rs61212815

Fonstad, M.A., Marcus, W.A., 2005. Remote sensing of stream depths with hydraulically assisted bathymetry (HAB) models. Geomorphology 72, 320–339. doi:10.1016/j.geomorph.2005.06.005

Frappart, F., Calmant, S., Cauhopé, M., Seyler, F., Cazenave, A., 2006. Preliminary results of ENVISAT RA-2-derived water levels validation over the Amazon basin. Remote Sens. Environ. 100, 252–264. doi:10.1016/j.rse.2005.10.027

Fujita, I., Hino, T., 2003. Unseeded and Seeded PIV Measurements of River Flows Videotaped from a Helicopter. J. Vis. 6, 245–252. doi:10.1007/BF03181465

Fujita, I., Kunita, Y., 2011. Application of aerial LSPIV to the 2002 flood of the Yodo River using a helicopter mounted high density video camera. J. Hydro-Environment Res. 5, 323–331. doi:10.1016/j.jher.2011.05.003

Giordano, F., Mattei, G., Parente, C., Peluso, F., Santamaria, R., 2015. Integrating sensors into a marine drone for bathymetric 3D surveys in shallow waters. Sensors 16. doi:10.3390/s16010041

Gondwe, B.R.N., Hong, S.H., Wdowinski, S., Bauer-Gottwein, P., 2010. Hydrologic dynamics of the ground-water-dependent Sian Ka'an wetlands, Mexico, derived from InSAR and SAR data. Wetlands 30, 1–13. doi:10.1007/s13157-009-0016-z

Guenther, G.., 1981. Accuracy and penetration measurements from hydrographic trials of the AOL system, in: Proc. 4th Laser Hydrography Symposium. Salisbury, pp. 108–150.

Guenther, G.C., 2001. Airborne Lidar Bathymetry, in: Digital Elevation Model Technologies and Applications. The DEM Users Manual. 8401 Arlington Blvd., p.

253-320 .

Hall, A.C., Schumann, G.J.P., Bamber, J.L., Bates, P.D., Trigg, M.A., 2012. Geodetic corrections to Amazon River water level gauges using ICESat altimetry. Water Resour. Res. 48. doi:10.1029/2011WR010895

Hamylton, S., Hedley, J., Beaman, R., 2015. Derivation of High-Resolution Bathymetry from Multispectral Satellite Imagery: A Comparison of Empirical and Optimisation Methods through Geographical Error Analysis. Remote Sens. 7, 16257–16273. doi:10.3390/rs71215829

Hauet, A., Creutin, J.-D., Belleudy, P., 2008. Sensitivity study of large-scale particle image velocimetry measurement of river discharge using numerical simulation. J. Hydrol. 349, 178–190. doi:10.1016/j.jhydrol.2007.10.062

Hilldale, R.C., Raff, D., 2008. Assessing the ability of airborne LiDAR to map river bathymetry. Earth Surf. Process. Landforms 33, 773–783. doi:10.1002/esp.1575

Hoffmann, H., Nieto, H., Jensen, R., Guzinski, R., Zarco-Tejada, P., Friborg, T., 2016. Estimating evaporation with thermal UAV data and two-source energy balance models. Hydrol. Earth Syst. Sci. 20, 697–713. doi:10.5194/hess-20-697-2016

Holm, B., Goosmann, R., 2016. Determining the surface velocity field of rivers from airborne video capture.

Hopkinson, C., Crasto, N., Marsh, P., Forbes, D., Lesack, L., 2011. Investigating the spatial distribution of water levels in the Mackenzie Delta using airborne LiDAR. Hydrol. Process. 25, 2995–3011. doi:10.1002/hyp.8167

Husson, E., Ecke, F., Reese, H., 2016. Comparison of Manual Mapping and Automated Object-Based Image Analysis of Non-Submerged Aquatic Vegetation from Very-High-Resolution UAS Images. Remote Sens. 8, 724. doi:10.3390/rs8090724

Irish, J., 1997. Using high-resolution bathymetry to determine sediment budgets: New Pass, Florida, in: New Insights Into Beach Preservation. FLORIDA SHORE & BEACH PRESERVATION ASSOCIATION, pp. 183–198.

Jodeau, M., Hauet, A., Paquier, A., Le Coz, J., Dramais, G., 2008. Application and evaluation of LS-PIV technique for the monitoring of river surface velocities in high flow conditions. Flow Meas. Instrum. 19, 117–127. doi:10.1016/j.flowmeasinst.2007.11.004

Kantoush, S. a, Schleiss, A.J., 2009. Channel formation during flushing of large shallow reservoirs with different geometries. Environ. Technol. 30, 855–63. doi:10.1080/09593330902990162

Kiel, B., Alsdorf, D., LeFavour, G., 2006. Capability of SRTM C- and X-band DEM Data to Measure Water Elevations in Ohio and the Amazon. Photogramm. Eng. Remote Sens. 72, 313–320. doi:10.14358/PERS.72.3.313

Kim, Y., Muste, M., Hauet, A., Krajewski, W.F., Kruger, A., Bradley, A., 2008. Stream discharge using mobile large-scale particle image velocimetry: A proof of concept. Water Resour. Res. 44. doi:10.1029/2006WR005441

Kinzel, P.J., Wright, C.W., Nelson, J.M., Burman, A.R., 2007. Evaluation of an Experimental LiDAR for Surveying a Shallow, Braided, Sand-Bedded River. J. Hydraul. Eng. 133, 838–842. doi:10.1061/(ASCE)0733-9429(2007)133:7(838)

Klemas, V. V., 2015. Coastal and Environmental Remote Sensing from Unmanned Aerial Vehicles: An Overview. J. Coast. Res. 315, 1260–1267. doi:10.2112/JCOASTRES-D-15-00005.1

Koblinsky, C., Clarke, R., 1993. Measurement of river level variations with satellite altimetry. Water Resour. Res. 29, 1839–1848. doi:Doi 10.1029/93wr00542

Lane, S.N., Widdison, P.E., Thomas, R.E., Ashworth, P.J., Best, J.L., Lunt, I.A., Sambrook Smith, G.H., Simpson, C.J., 2010. Quantification of braided river channel change using archival digital image analysis. Earth Surf. Process. Landforms 35, 971–985. doi:10.1002/esp.2015

Lee, K.R., Kim, A.M., Olsen, R.C., Kruse, F.A., 2011. Using WorldView-2 to determine bottom-type and bathymetry. Ocean Sens. Monit. III, April 26, 2011 - April 27 8030, The Society of Photo-Optical Instrumentation Engin. doi:10.1117/12.883578

LeFavour, G., Alsdorf, D., 2005. Water slope and discharge in the Amazon River estimated using the shuttle radar topography mission digital elevation model. Geophys. Res. Lett. 32, L17404. doi:10.1029/2005GL023836

Legleiter, C.J., Overstreet, B.T., 2012. Mapping gravel bed river bathymetry from space. J. Geophys. Res. Earth Surf. 117. doi:10.1029/2012JF002539

Legleiter, C.J., Roberts, D.A., 2005. Effects of channel morphology and sensor spatial resolution on image-derived depth estimates. Remote Sens. Environ. 95, 231–247. doi:10.1016/j.rse.2004.12.013

Lejot, J., Delacourt, C., Piégay, H., Fournier, T., Trémélo, M.-L., Allemand, P., 2007. Very high spatial resolution imagery for channel bathymetry and topography from an unmanned mapping controlled platform. Earth Surf. Process. Landforms 32, 1705–1725. doi:10.1002/esp.1595

Liceaga-Correa, M. a., Euan-Avila, J.I., 2002. Assessment of coral reef bathymetric mapping using visible Landsat Thematic Mapper data. Int. J. Remote Sens. 23, 3–14. doi:10.1080/01431160010008573

Lyons, M., Phinn, S., Roelfsema, C., 2011. Integrating Quickbird multi-spectral satellite and field data: Mapping bathymetry, seagrass cover, seagrass species and change in Moreton Bay, Australia in 2004 and 2007. Remote Sens. 3, 42–64. doi:10.3390/rs3010042

Lüthi, B., Philippe, T., Peña-Haro, S., 2014. Mobile device app for small open-channel flow measurement, in: 7th Intl. Congress on Env. Modelling and Software. pp. 283–287.

Lyzenga, D.R., 1981. Remote sensing of bottom reflectance and water attenuation parameters in shallow water using aircraft and Landsat data. Int. J. Remote Sens. 2, 71–82. doi:10.1080/01431168108948342

Lyzenga, D.R., Malinas, N.P., Tanis, F.J., 2006. Multispectral bathymetry using a simple physically based algorithm. IEEE Trans. Geosci. Remote Sens. 44, 2251–2259. doi:10.1109/TGRS.2006.872909

Maillard, P., Bercher, N., Calmant, S., 2015. New processing approaches on the retrieval of water levels in Envisat and SARAL radar altimetry over rivers: A case study of the São Francisco River, Brazil. Remote Sens. Environ. 156, 226–241. doi:10.1016/j.rse.2014.09.027

Mandlburger, G., Pfennigbauer, M., Wieser, M., Riegl, U., Pfeifer, N., 2016. Evaluation Of A Novel Uav-Borne Topo-Bathymetric Laser Profiler. ISPRS - Int. Arch. Photogramm. Remote Sens. Spat. Inf. Sci. XLI-B1, 933–939. doi:10.5194/isprs-archives-XLI-B1-933-2016

Meselhe, E.A., Peeva, T., Muste, M., 2004. Large Scale Particle Image Velocimetry for Low Velocity and Shallow Water Flows. J. Hydraul. Eng. 130, 937–940. doi:10.1061/(ASCE)0733-9429(2004)130:9(937)

Michailovsky, C.I., McEnnis, S., Berry, P.A.M., Smith, R., Bauer-Gottwein, P., 2012. River monitoring from satellite radar altimetry in the Zambezi River basin. Hydrol. Earth Syst. Sci. 16, 2181–2192. doi:10.5194/hess-16-2181-2012

Moramarco, T., Corato, G., Melone, F., Singh, V.P., 2013. An entropy-based method for determining the flow depth distribution in natural channels. J. Hydrol. 497, 176–188. doi:10.1016/j.jhydrol.2013.06.002

Morris, C.S., Gill, S.K., 1994a. Variation of Great Lakes water levels derived from Geosat altimetry. Water Resour. Res. 30, 1009–1017. doi:10.1029/94WR00064

Morris, C.S., Gill, S.K., 1994b. Evaluation of the TOPEX/POSEIDON altimeter system over the Great Lakes. J. Geophys. Res. 99, 24527. doi:10.1029/94JC01642

Muste, M., Hauet, A., Fujita, I., Legout, C., Ho, H.C., 2014. Capabilities of large-scale particle image velocimetry to characterize shallow free-surface flows. Adv. Water Resour. doi:10.1016/j.advwatres.2014.04.004

Neeck, S.P., Lindstrom, E.J., Vaze, P. V., Fu, L.-L., 2012. Surface Water and Ocean Topography (SWOT) mission, in: Conference on Sensors, Systems and Next-Generation Satellites XVI. p. 85330G. doi:10.1117/12.981151

Niedzielski, T., Witek, M., Spallek, W., 2016. Observing river stages using unmanned aerial vehicles. Hydrol. Earth Syst. Sci 20, 3193–3205. doi:10.5194/hess-20-3193-2016

O'Loughlin, F.E., Neal, J., Yamazaki, D., Bates, P.D., 2016. ICESat-derived inland water surface spot heights. Water Resour. Res. 52, 3276–3284. doi:10.1002/2015WR018237

Perry, G.J., 1999. Post-processing in laser airborne bathymetry systems, in: Proc. ROPME/PERSGA/IHB Workshop on Hydrographic Activities in the ROPME Sea Area and Red Sea.

Phan, V.H., Lindenbergh, R., Menenti, M., 2012. ICESat derived elevation changes of Tibetan lakes between 2003 and 2009. Int. J. Appl. Earth Obs. Geoinf. 17, 12–22. doi:10.1016/j.jag.2011.09.015

Philippe, T., Luethi, B., Peña-Haro, S., 2017. Mesure optique, et non-intrusive du débit des cours d'eau: quand le smartphone se transforme en débitmètre, in: Hydrométrie 2017, Lyon. SHF.

Plant, W.J., Keller, W.C., Hayes, K., 2005. Measurement of river surface currents with coherent microwave systems. IEEE Trans. Geosci. Remote Sens. 43, 1242–1257. doi:10.1109/TGRS.2005.845641

Raffel, M., Willert, C.E., Wereley, S.T., Kompenhans, J., 2007. Particle Image Velocimetry: A Practical Guide, Particle Image Velocimetry. doi:10.1097/JTO.0b013e3182370e69

Rantz, S.E., 1982. Measurement and Computation of Streamflow. Vol. 1 - Meas. Stage Discharge, USGS Water Supply Pap. 2175 Vol 1, 313. doi:10.1029/WR017i001p00131

Romeiser, R., Runge, H., Suchandt, S., Sprenger, J., Weilbeer, H., Sohrmann, A., Stammer, D., 2007. Current measurements in rivers by spaceborne along-track InSAR, in: IEEE Transactions on Geoscience and Remote Sensing. pp. 4019–4031. doi:10.1109/TGRS.2007.904837

Schumann, G., Matgen, P., Cutler, M.E.J.E.J., Black, A., Hoffmann, L., Pfister, L., 2008. Comparison of remotely sensed water stages from LiDAR, topographic contours and SRTM. ISPRS J. Photogramm. Remote Sens. 63, 283–296. doi:10.1016/j.isprsjprs.2007.09.004

Schumann, G.J.-P., Domeneghetti, A., 2016. Exploiting the proliferation of current and future satellite observations of rivers. Hydrol. Process. 30, 2891–2896. doi:10.1002/hyp.10825

Stumpf, R.P., Holderied, K., Sinclair, M., 2003. Determination of water depth with high-resolution satellite imagery over variable bottom types. Limnol. Oceanogr. 48, 547–556. doi:10.4319/lo.2003.48.1_part_2.0547

Sulistioadi, Y.B., Tseng, K.H., Shum, C.K., Hidayat, H., Sumaryono, M., Suhardiman, A., Setiawan, F., Sunarso, S., 2015. Satellite radar altimetry for monitoring small rivers and lakes in Indonesia. Hydrol. Earth Syst. Sci. 19, 341–359. doi:10.5194/hess-19-341-2015

Tamminga, a., Hugenholtz, C., Eaton, B., Lapointe, M., 2014. Hyperspatial Remote Sensing of Channel Reach Morphology and Hydraulic Fish Habitat Using an Unmanned Aerial Vehicle (Uav): a First Assessment in the Context of River Research and Management. River Res. Appl. n/a-n/a. doi:10.1002/rra.2743

Tauro, F., Pagano, C., Phamduy, P., Grimaldi, S., Porfiri, M., 2015a. Large-Scale Particle Image Velocimetry From an Unmanned Aerial Vehicle. IEEE/ASME Trans. Mechantronics 20, 1–7. doi:10.1109/TMECH.2015.2408112

Tauro, F., Petroselli, A., Porfiri, M., Giandomenico, L., Bernardi, G., Mele, F., Spina, D., Grimaldi, S., 2016a. A novel permanent gauge-cam station for surface-flow observations on the Tiber River. Geosci. Instrumentation, Methods Data Syst. 5, 241–251. doi:10.5194/gi-5-241-2016

Tauro, F., Petroselli, A., Arcangeletti, E., 2015b. Assessment of drone-based surface flow observations. Hydrol. Process. 30, 1114–1130. doi:10.1002/hyp.10698

Tauro, F., Porfiri, M., Grimaldi, S., 2016b. Surface flow measurements from drones. J. Hydrol. 540, 240–245. doi:10.1016/j.jhydrol.2016.06.012

Tauro, F., Porfiri, M., Grimaldi, S., 2014. Orienting the camera and firing lasers to enhance large scale particle image velocimetry for streamflow monitoring. Water Resour. Res. 50, 7470–7483. doi:10.1002/2014WR015952

Tazioli, A., 2011. Experimental methods for river discharge measurements: comparison among tracers and current meter. Hydrol. Sci. J. 56, 1314–1324. doi:10.1080/02626667.2011.607822

Thielicke, W., Stamhuis, E.J., 2014. PIVlab - Towards User-friendly, Affordable and Accurate Digital Particle Image Velocimetry in MATLAB. J. Open Res. Softw. 2,

e30. doi:10.5334/jors.bl

Virili, M., Valigi, P., Ciarfuglia, T., Pagnottelli, S., 2015. A prototype of radar-drone system for measuring the surface flow velocity at river sites and discharge estimation. Geophys. Res. Abstr. J. Hydr. Engrg. J. Hydrol. Eng. 17, 2015–12853.

Vousdoukas, M.I., Pennucci, G., Holman, R.A., Conley, D.C., 2011. A semi automatic technique for Rapid Environmental Assessment in the coastal zone using Small Unmanned Aerial Vehicles (SUAV). J. Coast. Res.

Vrugt, J.A., 2016. Markov chain Monte Carlo simulation using the DREAM software package: Theory, concepts, and MATLAB implementation. Environ. Model. Softw. 75, 273–316. doi:10.1016/j.envsoft.2015.08.013

Vrugt, J. a., ter Braak, C.J.F., Gupta, H. V., Robinson, B. a., 2008. Equifinality of formal (DREAM) and informal (GLUE) Bayesian approaches in hydrologic modeling? Stoch. Environ. Res. Risk Assess. 23, 1011–1026. doi:10.1007/s00477-008-0274-y

Watts, A.C., Ambrosia, V.G., Hinkley, E.A., 2012. Unmanned Aircraft Systems in Remote Sensing and Scientific Research: Classification and Considerations of Use. Remote Sens. 4(6), 1671–1692. doi:10.3390/rs4061671

Westaway, R.M., Lane, S.N., Hicks, D.M., 2001. Remote sensing of clear-water, shallow, gravel-bed rivers using digital photogrammetry. Photogramm. Eng. Remote Sensing 67, 1271–1281.

Winterbottom, S.J., Gilvear, D.J., 1997. Quantification of channel bed morphology in gravel-bed rivers using airborne multispectral imagery and aerial photography. Regul. Rivers-Research Manag. 13, 489–499. doi:10.1002/(SICI)1099-1646(199711/12)13:6<489::AID-RRR471>3.0.CO;2-X

Woodget, A.S., Carbonneau, P.E., Visser, F., Maddock, I.P., 2015. Quantifying submerged fluvial topography using hyperspatial resolution UAS imagery and structure from motion photogrammetry. Earth Surf. Process. Landforms 40, 47–64. doi:10.1002/esp.3613

Yorke, T.H., Oberg, K.A., 2002. Measuring river velocity and discharge with acoustic Doppler profilers. Flow Meas. Instrum. 13, 191–195. doi:10.1016/S0955-5986(02)00051-1

9 Papers

I **Bandini, F.**, Jakobsen, J., Olesen, D., Reyna-Gutierrez, J. A., and Bauer-Gottwein, P. (2017). "Measuring water level in rivers and lakes from lightweight Unmanned Aerial Vehicles." *Journal of Hydrology*, 548, 237–250

II **Bandini, F.**, Butts, M., Vammen Torsten, J., and Bauer-Gottwein, P. (2017). "Water level observations from Unmanned Aerial Vehicles for improving estimates of surface water-groundwater interaction". *In print-Hydrological Processes*.

III **Bandini, F.**, Olesen, D., Jakobsen, J., Kittel, C. M. M., Wang, S., Garcia, M., and Bauer-Gottwein, P. (2017). "River bathymetry observations from a tethered single beam sonar controlled by an Unmanned Aerial Vehicle." *Manuscript under review.*

IV **Bandini, F.**, Lopez-Tamayo, A., Merediz-Alonso, G., Olesen, D., Jakobsen, J., Wang, S., Garcia, M., and Bauer-Gottwein, P. (2017). "Unmanned Aerial Vehicle observations of bathymetry and water level in the cenotes and lagoons of the Yucatan Peninsula". *Manuscript under review.*

TEXT FOR WWW-VERSION (with out papers)

In this online version of the thesis, **paper I-IV** are not included but can be obtained from electronic article databases e.g. via www.orbit.dtu.dk or on request from.

DTU Environment
Technical University of Denmark
Miljoevej, Building 113
2800 Kgs. Lyngby
Denmark

info@env.dtu.dk.

"The Department of Environmental Engineering (DTU Environment) conducts science based engineering research within six sections: Water Resources Engineering, Water Technology, Urban Water Systems, Residual Resource Engineering, Environmental Chemistry and Atmospheric Environment.

The department dates back to 1865, when Ludvig August Colding, the founder of the department, gave the first lecture on sanitary engineering as response to the cholera epidemics in Copenhagen in the late 1800s."

Department of Environmental Engineering
Technical University of Denmark

DTU Environment
Bygningstorvet, building 115
2800 Kgs. Lyngby
Tlf. +45 4525 1600
Fax +45 4593 2850

www.env.dtu.dk